Pramāṇa, Vol. 19, No. 6, December 1982, pp. 593-632. © Printed in India.

Neutron, x-ray and lattice dynamical studies of paraelectric Sb_2S_3

K R RAO, S L CHAPLOT, V M PADMANABHAN* and P R VIJAYARAGHAVAN
Nuclear Physics Division, Bhabha Atomic Research Centre, Trombay, Bombay 400 085, India
*Neutron Physics Division

MS received 24 May 1982

Abstract. Neutron and x-ray diffraction studies of Sb_2S_3 indicate extensive diffuse scattering in the plane perpendicular to the chain axis of polymer-like $(Sb_4S_6)_n$ molecules. The crystal structure of the paraelectric phase is said to be orthorhombic with space group D_{2h}^{16} with four molecules per unit cell. The observed diffuse scattering may be due to static disorder or some dynamical effects. In this paper the authors have examined the possible dynamical origin by recourse to lattice dynamical studies. Dispersion relation of phonons along the three symmetry directions a^*, b^* and c^* is evaluated based on a lattice dynamical model incorporating Coulomb, covalent and a Born-Mayer-like short range interactions. Group theoretical analysis based on the group of neutral elements of crystal sites (GNES) was essential in order to examine and aid in the numerical computations. The group theoretical technique involving GNES extended to 'pseudo-molecular' systems is also discussed in this context.

The phonon dispersion relation shows that there are rather flat TA-TO branches of very low frequency in the a and c directions which may give rise to diffuse scattering. The branches along the b-axis are quite dissimilar to those along a and c axes because of anisotropy. Variation of the potential parameters leads to instability of the lowest TA-TO branch. This is suggestive of a temperatures or pressure-dependent phase transition. However since these modes are optically 'silent' one needs to carry out either high resolution neutron scattering or ultrasonic studies to confirm various aspects of the theoretical studies.

Keywords. Antimony trisulphide; lattice dynamics; phase transitions; neutron diffraction; x-ray diffraction; paraelectric Sb_2S_3.

1. Introduction

One and two-dimensional materials have been subjects of investigation during the last decade to understand their various anisotropic properties. Physically they behave as fibrous or as layer-like crystals; mechanically and electronically they have large variations as a result of anisotropy. Light scattering techniques, x-ray diffraction and neutron scattering techniques have been used to study a variety of these systems (Wieting and Schluter 1979). New families of the low-dimensional systems are being discovered and getting investigated.

The V-VI-VII compounds like the sulfoiodide SbSI and V_2VI_3 compounds (sesquichalcogenides) like Sb_2S_3 have been of interest since they not only exhibit low-dimensional features but also because they are semiconductors exhibiting other unusual properties like photoconductivity, pyroelectricity and ferroelectricity (Bohac and Kaufmann 1975; Grigas 1978; Fridkin 1980). In fact the two systems SbSI and Sb_2S_3 have close similarities to each other since they have chain-like structure

and crystallise with the same space group D_{2h}^{16} with four molecules per unit cell in the paraelectric phase. Sb_2S_3 also has some semblance to members of another family of layered crystals, namely As_2S_3, etc. which have attracted lot of interest due to their semiconducting properties in their crystalline and amorphous states.

SbSI and Sb_2S_3 have been studied extensively by infrared and Raman scattering techniques. Neutron inelastic scattering technique has been used in investigating SbSI. Sb_2S_3 has not been studied so far by neutron techniques, which would be helpful to determine the dynamics of the system completely. So also, detailed lattice dynamical calculations have not been carried out to interpret light scattering and neutron data either in SbSI or Sb_2S_3. We took up recently experimental and theoretical investigations of Sb_2S_3 and report in this paper results of our investigations. In § 2 we describe details of crystal structure of Sb_2S_3. Section 3 deals with group-theoretical analysis of lattice vibrations of this system. We have used the group of neutral elements of a site for this analysis. In this connection we have discussed how this approach can be used for a 'molecular' system. Results from group theory were essential to help in numerical calculations reported in the later sections. Elastic and inelastic neutron scattering results and results from x-ray diffraction are outlined in § 4. Lattice dynamical calculations based on a model involving covalent, Coulomb and short range (repulsive) two-body interactions are reported in § 5. Section 6 deals with interpretation of the experimental observations using the results of lattice dynamical calculations. We shall discuss lattice dynamical aspects of SbSI in a forthcoming paper.

2. Structure of stibnite (Sb_2S_3)

At room temperature, the mineral stibnite (chemical composition Sb_2S_3) crystallises in orthorhombic form with four molecules per unit cell (Hoffmann 1933; Wyckoff 1948; Scavnicar 1960; Bayliss and Nowacki 1972; McKee and McMullan 1975). The space group can be referred to as D_{2h}^{16} (*Pnma*)* with the atomic positions given by,

$$4c: \pm (v, \tfrac{1}{4}, u), \pm (v + \tfrac{1}{2}, \tfrac{1}{4}, \tfrac{1}{2} - u)$$

The parameters v and u are given in table 1(a) and the atomic positions of all the

Table 1(a). Atomic coordinate parameters in Sb_2S_3 (from Bayliss and Nowacki 1972).

Atom	v	u
Sb_I	0·0293	0·3261
Sb_{II}	0·3505	0·5360
S_I	0·0497	0·8769
S_{II}	0·8749	0·5614
S_{III}	0·2079	0·1917

*Both Hoffmann (1933) and Scavnicar (1960) note that in the x-ray diffraction studies there are systematic absence of (*hol*)-for $h + l$ odd-and (*okl*)-for k and l odd-reflections. In the orthorhombic system these extinctions are consistent with *Pbmn* (D_{2h}^{16}) and *Pbn*2_1 (C_{2v}^{9}) space groups. However, they conclude that *Pbnm* is the most probable space group on the basis of morphology, lack of pyroelectric effect and etching figures-all indicating a centrosymmetric space group. This observation is also said to be supported by the exact correspondence between intensities of (*hko*) and (*hk*2) reflections.

twenty atoms in the unit cell are listed in table 1(b) for ready reference. The crystal structure is shown in figure 1. Lattice constants as given by different experimenters are given in table 1(c). We have used the lattice constants and atomic co-ordinate parameters as given by Bayliss and Nowacki (1972) for the lattice dynamical calculations.**

Following Scavnicar (1960) the structure may be described essentially as consisting of several ribbons of $(Sb_4S_6)_n$ forming sheets infinitely extended parallel to *b* axis. In each sheet each antimony and each sulphur is surrounded by three atoms of the opposite kind. In the three-dimensional configuration, it may be noted that one half of the Sb atoms (referred to as Sb_{II}) are surrounded by five S atoms (S_{III}) each

Table 1(b). Labelling and coordinates of all atoms in the unit cell.

Atom No.	Molecule No.	Atomic Species	Atomic Type No.	Molecule Type No.	Fractional coordinates *x*	*y*	*z*
1	1	Sb_I	1	1	0·0293	0·25	0·3261
2		Sb_{II}	2		0·1495	0·75	0·0360
3		S_I	3		0·9503	0·75	0·1231
4		S_{II}	4		0·1251	0·75	0·4386
5		S_{III}	5		0·2079	0·25	0·1917
6	2	Sb_I	1	1	0·5293	0·25	0·1739
7		Sb_{II}	2		0·6495	0·75	0·4640
8		S_I	3		0·4503	0·75	0·3769
9		S_{II}	4		0·6251	0·75	0·0614
10		S_{III}	5		0·7079	0·25	0·3083
11	3	Sb_I	1	1	0·9707	0·75	0·6739
12		Sb_{II}	2		0·8505	0·25	0·9640
13		S_I	3		0 0497	0·25	0·8769
14		S_{II}	4		0·8749	0·25	0·5614
15		S_{III}	5		0·7921	0·75	0·8083
16	4	Sb_I	1	1	0·4707	0·75	0·8201
17		Sb_{II}	2		0·3505	0·25	0·5360
18		S_I	3		0·5497	0·25	0·6231
19		S_{II}	4		0·3749	0·25	0·9386
20		S_{III}	5		0·2921	0·75	0·6917

Table 1(c). Lattice constants of Sb_2S_3.

a	*b*	*c*	Reference
11·28kx	3·83	11·20	Hoffmann (1933)
11·310Å	3·8389	11·299	Wyckoff (1958)
11·33(2)	3·84(1)	11·25	Scavnicar (1960)
11·3107(9)	3·8363	11·2285	Bayliss and Nowacki (1972)
11·3018	3·8341	11·2271	McKee and McMullan (1975)

**It should be pointed out however that we have noted that the literature dealing with study of macroscopic properties and optical spectra lead to contradictions regarding space group of the crystal in various temperature ranges as described in appendix 1. However the high temperature phase is believed to be paraelectric having space group D_{2h}^{16} with four molecules per unit cell. In view of small changes that may occur in lattice constants as a function of temperature, we believe that results of our studies of paraelectric phase would still be useful irrespective of the paraelectric to ferroelectric phase transition temperature.

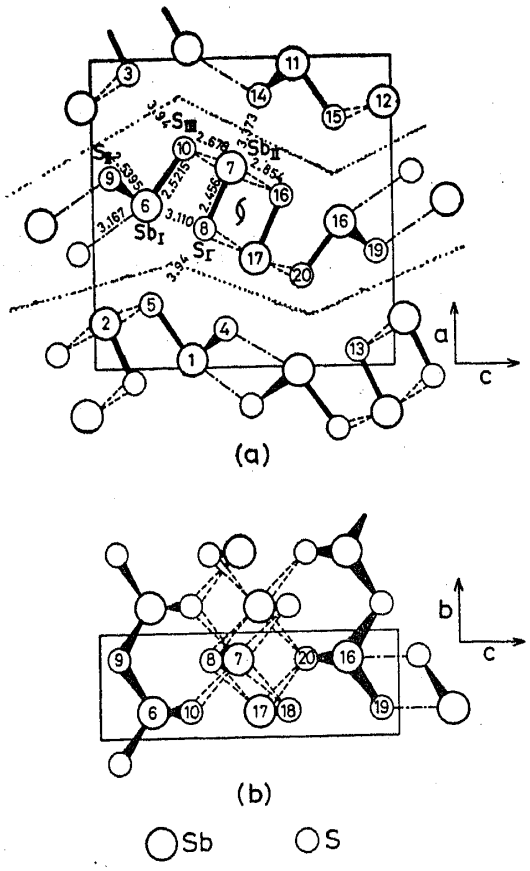

Figure 1. Crystal structure of Sb_2S_3 projected on to ac plane in (a) and on to bc plane in (b). Interatomic pairs considered to be covalently interacting in the lattice dynamical model are joined by dark bars. Dotted lines indicate cleavage planes as per mineralogy. In (b), projection of only the atoms in the central Sb_4S_6 unit is shown. The numbering corresponds to atomic labeling given in Table 1(b).

of these S atoms being linked to the Sb atoms. The other half of the Sb atoms (Sb_I) and remaining S atoms (S_I and S_{II}) exhibit trivalency and bivalency respectively. The coordination polyhedra for five-coordinated Sb is a square pyramid, the Sb atom being slightly displaced outwards of the pyramid base. As pointed out by Scavnicar (1960), there are two types of bondings in the crystal as indicated by the bond lengths. There are shorter bonds of Sb-S separations 2.46 to 2.85 Å which may be considered to be strong. These bonds help to group one half of the contents of the unit cell (four Sb atoms and six S atoms) together. The arrangement of the atoms in this group allows a $\langle 010 \rangle$ 2-fold screw axis at its centre. Symmetry operation of this screw axis results in the formation of the infinite $(Sb_4S_6)_n$ ribbon or chain parallel to the *b* axis. The *b*-axis, therefore, turns out to be a unique axis in the system, sometimes referred to as needle axis or chain axis. The ribbon-like $(Sb_4S_6)_n$ polymers related by the 2-fold screw axes at $(\frac{1}{2}00)$ or $(00\frac{1}{2})$ can be regarded as forming a zig-zag sheet which is roughly perpendicular to the *a*-axis. These sheets give rise to description of the crystal as a layered crystal (Wieting and Schulter 1979). The second type of bondings typified by Sb_I-S_{II} distances of nearly 3.17 Å and much weaker Sb-S interactions at distances of 3.37 Å and 3.94 Å bind the ribbons into vertical sheets and these sheets into a three-dimensional network.

3. Group theoretical aspects of dynamics of Sb_2S_3

3.1 *General aspects*

Maradudin and Vosko (1968) and Venkataraman and Sahni (1970) have outlined methods of studying symmetry aspects of lattice dynamics of atomic and 'molecular' systems. Recently Sieskind (1978) has pointed out that one can make use of site symmetry to simplify group theoretical analysis further. He has shown that the matrices associated with reducible multiplier representations $\{T(\mathbf{q}, S)\}$, corresponding to various space group operations $\{S\}$ of the crystal that constitute the group of the wavevector $G_0(\mathbf{q})$, $\mathbf{q}$ being a wavevector of phonons, separate into as many independent square matrices $\boldsymbol{T}_p(\mathbf{q}, S)$ as the elementary cell holds various homologous 'ions'. With respect to $\boldsymbol{T}(\mathbf{q}, S)$, the crystal appears as a combination of sub-crystals formed by homologous ions which reside at the homologous sites. Sieskind (1978) has shown that the $\boldsymbol{T}_p(\mathbf{q}, S)$ matrices may be classified into classes of formally identical matrices called isostructural matrices. These classes are derived from consideration of so-called 'group of neutral elements of crystalline sites (GNES)'. Such a description allows one to build easily the projection operators $\hat{P}$ needed for reduction of the dynamical matrix to block diagonal form. We have followed the method of Sieskind (1978) as it helps in analysing the problem considerably and elegantly. Whereas Sieskind's paper deals with atomic case only, we discuss first how the scheme can be adopted for 'molecular' systems. In the subsection 3.5 (v) dealing with reduction of dynamical matrix, we have outlined how one can consider equivalent and non-equivalent atom-pairs to arrive at the structure of the dynamical matrix in this scheme. The results of particular interest to us are (i) the structure of the dynamical matrix to check against numerical results and (ii) symmetry vector matrices needed for block diagonalisation of dynamical matrices for simplifying the eigenvalue problem.

The primitive translation vectors of the orthorhombic lattice of Sb_2S_3 are defined by $\mathbf{a}_1 = a\mathbf{i}$, $\mathbf{a}_2 = b\mathbf{j}$ and $\mathbf{a}_3 = c\mathbf{k}$ where $\mathbf{i}$, $\mathbf{j}$ and $\mathbf{k}$ are unit orthogonal vectors and a, b and c are cell dimensions along these directions. The reciprocal lattice is also orthorhombic; the reciprocal lattice vectors are given by $\mathbf{b}_1 = (2\pi/a)\,\mathbf{i}$, $\mathbf{b}_2 = (2\pi/b)\,\mathbf{j}$ and $\mathbf{b}_3 = (2\pi/c)\mathbf{k}$. The Brillouin zone is shown in figure 2. The symmetry operations of the space group D_{2h}^{16} are given in table 2. The point group operations associated with this spacegroup are h_1, h_2, h_3, h_4, h_{25}, h_{26}, h_{27} and h_{28} in Kovalev (1965)'s notation. The space group operations decompose into a direct product of two groups one of which contains only the symmorphic group associated with h_1 and h_{25}

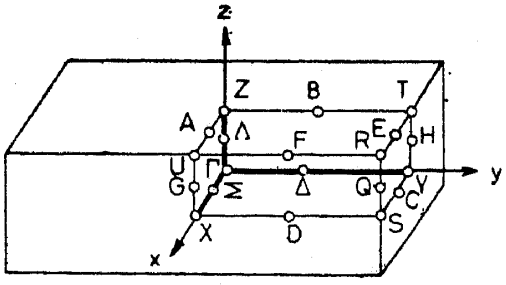

Figure 2. Brillouin zone of orthorhombic lattice.

and another non-symmorphic group associated with h_1, h_2, h_3 and h_4. That is

$$D_{2h}^{16}: (h_1, h_{25}) \otimes (h_1, h_2, h_3, h_4),$$

$$: (h_1, h_{25}) \otimes (h_1, h_2) \otimes (h_1, h_4).$$

The generators of the D_{2h}^{16} group may be chosen as h_{25}, h_2 and h_4. Under the effect of space group operations the atoms in the unit cell get exchanged or are left invariant and this can be determined by examining the coordinates of the transformed atom $\begin{pmatrix} L \\ K \end{pmatrix}$, starting from an atom $\begin{pmatrix} l \\ k \end{pmatrix}$ using the equation,

$$\mathbf{x}\begin{pmatrix} L \\ K \end{pmatrix} = S\,\mathbf{x}\begin{pmatrix} l \\ k \end{pmatrix} = S\,\mathbf{x}\begin{pmatrix} l \\ k \end{pmatrix} + \mathbf{v}\,(S). \tag{1}$$

Table 3(a) shows the effect of symmetry operations on the twenty atoms in the unit cell in terms of the atom labels given in column 1 of table 1(b).

Discussion of group theoretical aspect of crystalline lattices hinges on the construction of the reducible multiplier representation $\{T(\mathbf{q}, S)\}$ of the space group

Table 2. Symmetry operations of the space group D_{2h}^{16}.

Operation	Seitz's Notation	Kovalev's Notation	Effect of point group on (xyz)	Matrix Representation	Character
S_1	E/(000)	h_1	(xyz)	$\begin{vmatrix} 1 & 0 & 0 \\ 0 & 1 & 0 \\ 0 & 0 & 1 \end{vmatrix}$	3
S_2	$C_2(x)/(\frac{1}{2}, \frac{1}{2}, \frac{1}{2})$	h_2	$(x\bar{y}\bar{z})$	$\begin{vmatrix} 1 & 0 & 0 \\ 0 & -1 & 0 \\ 0 & 0 & -1 \end{vmatrix}$	-1
S_3	$C_2(y)/(0, \frac{1}{2}, 0)$	h_3	$(\bar{x}y\bar{z})$	$\begin{vmatrix} -1 & 0 & 0 \\ 0 & 1 & 0 \\ 0 & 0 & -1 \end{vmatrix}$	-1
S_4	$C_2(z)/(0, 0, \frac{1}{2})$	h_4	$(\bar{x}\bar{y}z)$	$\begin{vmatrix} -1 & 0 & 0 \\ 0 & -1 & 0 \\ 0 & 0 & 1 \end{vmatrix}$	-1
S_5	I/(0, 0, 0)	h_{25}	$(\bar{x}\bar{y}\bar{z})$	$\begin{vmatrix} -1 & 0 & 0 \\ 0 & -1 & 0 \\ 0 & 0 & -1 \end{vmatrix}$	-3
S_6	$\sigma_x/(\frac{1}{2}, \frac{1}{2}, \frac{1}{2})$	h_{26}	$(\bar{x}yz)$	$\begin{vmatrix} -1 & 0 & 0 \\ 0 & 1 & 0 \\ 0 & 0 & 1 \end{vmatrix}$	1
S_7	$\sigma_y/(0, \frac{1}{2}, 0)$	h_{27}	$(x\bar{y}z)$	$\begin{vmatrix} 1 & 0 & 0 \\ 0 & -1 & 0 \\ 0 & 0 & 1 \end{vmatrix}$	1
S_8	$\sigma_z/(\frac{1}{2}, 0, \frac{1}{2})$	h_{28}	$(xy\bar{z})$	$\begin{vmatrix} 1 & 0 & 0 \\ 0 & 1 & 0 \\ 0 & 0 & -1 \end{vmatrix}$	1

operations $\{S\}$. The most general form of the matrix $\boldsymbol{T}(\mathbf{q}, S)$ is given by* (Rao *et al* 1978, referred to hereafter as Paper I),

$$T^{ii'}_{\alpha\beta}(\mathbf{q}, \kappa\kappa', S) = C^i(S)\,\delta_{ii'}\,S_{\alpha\beta}\,\delta[\kappa, F_0(\kappa', S)]\,\exp\,[i\mathbf{G}\cdot\{\mathbf{x}(\kappa) - \mathbf{v}(S)\}] \quad (2)$$

applicable in external mode formalism. i and i' correspond to translation and rotation t and r of the constituent units. $C^i(S)=1$ for $i=t$; $C^i(S)=\|\boldsymbol{S}\|$ for $i=r$. α and β refer to cartesian components. $S_{\alpha\beta}$ is an element of the rotational matrix $\boldsymbol{S}$ associated with the operator S, $\mathbf{q}$ is any wavevector of the lattice, $v(S)$ the fractional translation associated with the operator. If unit κ is permuted with κ' under symmetry operation S, $\delta[\kappa, F_0(\kappa', S)]=1$; otherwise it is zero.

Table 3(a). Effect of symmetry operation on atoms in unit cell.

Atom No. (see Table 1(b)),	gets transformed to atom no. given here under effect of							
	S_1	S_2	S_3	S_4	S_5	S_6	S_7	S_8
1	1	6	11	16	11	16	1	6
2	2	7	12	17	12	17	2	7
3	3	8	13	18	13	18	3	8
4	4	9	14	19	14	19	4	9
5	5	10	15	20	15	20	5	10
6	6	1	16	11	16	11	6	1
7	7	2	17	12	17	12	7	2
8	8	3	18	13	18	13	8	3
9	9	4	19	14	19	14	9	4
10	10	5	20	15	20	15	10	5
11	11	16	1	6	1	6	11	16
12	12	17	2	7	2	7	12	17
13	13	18	3	8	3	8	13	18
14	14	19	4	9	4	9	14	19
15	15	20	5	10	5	10	15	20
16	16	11	6	1	6	1	16	11
17	17	12	7	2	7	2	17	12
18	18	13	8	3	8	3	18	13
19	19	14	9	4	9	4	19	14
20	20	15	10	5	10	5	20	15

Table 3(b). Effect of symmetry operations on 'pseudomolecules' in the unit cell.

'pseudo-molecule' no.	gets transformed into 'pseudomolecule' no. given here under symmetry operation							
	S_1	S_2	S_3	S_4	S_5	S_6	S_7	S_8
1	1	2	3	4	3	4	1	2
2	2	1	4	3	4	3	2	1
3	3	4	1	2	1	2	3	4
4	4	3	2	1	2	1	4	3

*The form of $\boldsymbol{T}(\mathbf{q}, S)$ given here differs from that given by Venkataraman and Sahni (1970) by a phase factor. The form given in (2) is appropriate from the point of view of commutability with dynamical matrix $\boldsymbol{M}(\mathbf{q})$ given later.

3.2 *Simplifications introduced by* GNES

The matrix $\boldsymbol{T}(\mathbf{q}, S)$ can be written symbolically as

$$\boldsymbol{T}(\mathbf{q}, S) = \boldsymbol{S}^{(3)} \otimes \boldsymbol{T}^{j}(\mathbf{q}, S), \tag{3}$$

a tensor product of two tensors, $S^{(3)}$ of dimensions 3 and $\boldsymbol{T}^{j}(\mathbf{q}, S)$ of j-dimensional Euclidean space; $j=v+2\mu$ where v refers to number of atoms and μ number of 'molecules' in the unit cell. We note that even if one cannot consider a set of atoms as forming a 'molecule' from the point of view of rigidity of the cluster as a whole, one can still use the fact that if a set of atoms is transformed from site to site without any interchange of atoms amongst themselves, such a group may still be identified as a 'molecule' for group theoretical purposes as it would result in considerable simplifications in group theoretical analysis. Specifically, simplifications will result by adopting a 'molecular' view in such cases even if we are interested in developing a strictly atomic model of dynamics. We wish to adopt an atomic model of lattice dynamics for Sb_2S_3 as there are no indications spectroscopically to allow us to treat Sb_2S_3 as a rigid unit. But Sb_2S_3 can be treated as a molecular unit for group theoretical analysis since the space group operations do not interchange any of the constituent atoms in this loosely bound (non-rigid) cluster. In order to avoid any confusion with truly 'molecular' units, henceforth we shall designate the non-rigid clusters, which can be treated as units for group theoretical purposes as 'pseudo-molecules'. We generalise Seiskind's approach to external mode formalism for group theoretical analysis.

If p_1 and p_2 identify atoms and 'molecules' in the unit cell and if $n(p_1)$ and $n(p_2)$ be the number of homologous crystalline atomic and 'molecular' sites of type p_1 and p_2 making C_{p_1} and C_{p_2} distinct families in the unit cell, $\boldsymbol{T}^{j}(\mathbf{q}, S)$ can be written as a direct sum of $n(p_1)$ and $n(p_2)$ dimensional square matrices $\boldsymbol{T}_{p_1}(\mathbf{q}, S)$ and $\boldsymbol{T}_{p_2}(\mathbf{q}, S)$ of general element $\boldsymbol{T}_{p}(\kappa\kappa', \mathbf{q}, S)$ ($p=p_1$ or p_2)

$$\boldsymbol{T}^{j}(\mathbf{q}, S) = \sum_{p_1=1}^{C_{p_1}\oplus} \boldsymbol{T}_{p_1}(\mathbf{q}, S) \oplus \sum_{p_2=1}^{C_{p_2}\oplus} \boldsymbol{T}_{p_2}(\mathbf{q}, S) \tag{4}$$

For Sb_2S_3, assuming 'pseudo-molecular' nature, $p_1=0$, $p_2=1$, $n(p_1)=0$ and $n(p_2)=4$. Therefore,

$$\boldsymbol{T}^{(4)}(\mathbf{q}, S) = \sum_{p_2=1}^{1\oplus} \boldsymbol{T}_{p_2}(\mathbf{q}, S) \equiv \underset{4\times 4}{\boldsymbol{T}_1}(\mathbf{q}, S). \tag{5}$$

We now examine the $\boldsymbol{T}_p(\mathbf{q}, S)$ matrices of the homologous sites p. The discussion follows essentially the approach of Sieskind (1978). As already indicated, p could be either p_1 or p_2. Equation (1) shows that κ' results from κ as a result of the space group operation S. Hence each operation S is a permutation operation and $\boldsymbol{T}_p(\mathbf{q}, S)$, matrices associated with S for any $\mathbf{q}$ are each related to a permutation matrix $\boldsymbol{T}_p(S)$ which is derived from $\boldsymbol{T}_p(\mathbf{q}, S)$ by replacing each non-zero element in the matrix

$\boldsymbol{T}_p(\mathbf{q}, S)$ by unity. Two different matrices $\boldsymbol{T}_p(\mathbf{q}, S)$ and $\boldsymbol{T}_p(\mathbf{q}, S')$ leading to the same permutation matrix are termed isostructural matrices. One can show that the $\boldsymbol{T}_p(\mathbf{q}, S)$ matrices arrange themselves in equivalent classes of isostructural matrices. The set $N(p)$ of operators in the space group G which leave invariant all the homologous sites of type p is called GNES. Consequently for all $S \in N(p)$, $\boldsymbol{T}_p(S)$ is the identity matrix. Furthermore, $N(p)$ makes a partition of the operators in G, into a collection of cosets of $N(p)$. So with each element of the factor group is associated a permutation matrix $\boldsymbol{T}_p(S_{\pi,\sigma})$, $(\pi=\text{I, II,}\ldots,f)$, $(\sigma=1, 2,\ldots, g_{N(p)})$. The order of the factor group $G/N(p)$ gives the number f of distinct permutation matrices; for the site p, $f=g/g_{N(p)}$, where g and $g_{N(p)}$ represent the order of the groups G and $N(p)$ respectively. For Sb_2S_3, $N(p_2)$; $\{h_1, h_{27}\}$; $p_2=1$; $f=g/g_{N(p_2)}=8/2=4$. Therefore, there are four different classes of matrices $\boldsymbol{T}_1(S_{\pi,\sigma})$, $\pi=$I, II, III, IV and $\sigma=1, 2$. $\boldsymbol{T}_1(S)$ indicates a permutation matrix of type $p_2=1$ corresponding to the operation S. In writing the $\boldsymbol{T}_1(S_{\pi,\sigma})$ matrices we resort to a simplified notation, namely we write only the permutation aspect of the 'pseudo-molecule' by writing unity instead of $\delta_{ii'}\, C^i(S)$ which occurs in (2). We adopt this procedure because we wish to use only the atomic model for lattice dynamics of Sb_2S_3. If one wishes to examine the external modes of a true 'molecular' system, terms $\delta_{ii'}\, C^i(S)$ have to be retained in $\boldsymbol{T}_{p_2}(S)$.

In table 4 we have given correspondence between operations that belong to different classes of GNES in terms of $S_{\pi,\sigma}$ and in Kovalev (1965)'s notation. Table 5 gives explicitly the permutation matrices $\boldsymbol{T}_1(S_{\pi,\sigma})$ for Sb_2S_3. We note that $\boldsymbol{T}_1(S_{\pi,\sigma})$ is independent of $\mathbf{q}$ and σ.

Table 4. Correspondence between labels $S_{\pi,\sigma}$ and Kovalev's notation.

Class π	I		II		III		IV	
GNES label σ	1	2	1	2	1	2	1	2
S	$S_{\text{I},1}$	$S_{\text{I},2}$	$S_{\text{II},1}$	$S_{\text{II},2}$	$S_{\text{III},1}$	$S_{\text{III},2}$	$S_{\text{IV},1}$	$S_{\text{IV},2}$
Kovalev's	h_1	h_{27}	h_2	h_{28}	h_3	h_{25}	h_4	h_{26}

Table 5. Permutation matrices $T_1(S_{\pi,\sigma})$ for Sb_2S_3 ($\sigma = 1$ and 2).

(a) Class (π =)I : $\{h_1, h_{27}\} = S_{\text{I},\sigma}$

$$\boldsymbol{T}_1(S_{\text{I},\sigma}) = \begin{vmatrix} 1 & 0 & 0 & 0 \\ 0 & 1 & 0 & 0 \\ 0 & 0 & 1 & 0 \\ 0 & 0 & 0 & 1 \end{vmatrix}$$

(b) Class II: $\{h_2, h_{28}\}$

$$\boldsymbol{T}_1(S_{\text{II},\sigma}) = \begin{vmatrix} 0 & 1 & 0 & 0 \\ 1 & 0 & 0 & 0 \\ 0 & 0 & 0 & 1 \\ 0 & 0 & 1 & 0 \end{vmatrix}$$

(c) Class III: $\{h_3, h_{25}\}$

$$\boldsymbol{T}_1(S_{\text{III},\sigma}) = \begin{vmatrix} 0 & 0 & 1 & 0 \\ 0 & 0 & 0 & 1 \\ 1 & 0 & 0 & 0 \\ 0 & 1 & 0 & 0 \end{vmatrix}$$

(d) Class IV: $\{h_4, h_{26}\}$

$$\boldsymbol{T}_1(S_{\text{IV},\sigma}) = \begin{vmatrix} 0 & 0 & 0 & 1 \\ 0 & 0 & 1 & 0 \\ 0 & 1 & 0 & 0 \\ 1 & 0 & 0 & 0 \end{vmatrix}$$

3.3. *The projection operator* $\hat{P}$.

The projection operator $\hat{P}$ is defined by

$$\mathbf{P}_{\mu\mu'}(\mathbf{q}, \lambda) = \frac{d_\lambda}{h} \sum_{S_n} \tau^*_{\mu\mu'}(\mathbf{q}, \lambda, S_n)\, \boldsymbol{T}(\mathbf{q}, S_n) \tag{6}$$

where $\tau_{\mu\mu'}(\mathbf{q}, \lambda, S_n)$ is the matrix element of the irreducible representations $\{\tau_\lambda\}$ associated with $G_0(\mathbf{q})$ for the operation $S_n (S_n \in G_0(\mathbf{q}))$.

$$\mathbf{P}_{\mu\mu'}(\mathbf{q}, \lambda) = \frac{d_\lambda}{h} \sum_{S_n} \tau^*_{\mu\mu'}(\mathbf{q}, \lambda, S_n) \{\boldsymbol{S}_n^{(3)} \otimes \boldsymbol{T}^j(\mathbf{q}, S_n)\} \tag{7}$$

$$= \frac{d_\lambda}{h} \sum_{\pi=1}^{f} \left\{ \sum_{\sigma=1}^{g_{N(p_1)}} \tau^*_{\mu\mu'}(\mathbf{q}, \lambda, S_{\pi,\sigma}) \{\boldsymbol{S}_\sigma^{(3)} \otimes \boldsymbol{T}_{p_1}(\mathbf{q}, S)\} \right.$$

$$\left. \oplus \sum_{\sigma=1}^{g_{N(p_2)}} \tau^*_{\mu\mu'}(\mathbf{q}, \lambda, S_{\pi,\sigma}) \{\boldsymbol{S}_\sigma^{(3)} \otimes \boldsymbol{T}_{p_2}(\mathbf{q}, S_\pi)\} \right.$$

$$= \frac{d\lambda}{h} \sum_{\pi=1}^{f} \left\{ \sum_{\sigma=1}^{g_{N(p_1)}} \tau^*_{\mu\mu'}(\mathbf{q}, \lambda, S_{\pi,\sigma})\, \boldsymbol{S}_\sigma^{(3)} \right\} \otimes \boldsymbol{T}_{p_1}(\mathbf{q}, S_\pi)$$

$$\oplus \left\{ \sum_{\sigma=1}^{g_{N(p_2)}} \tau^*_{\mu\mu'}(\mathbf{q}, \lambda, S_{\pi,\sigma})\, \boldsymbol{S}_\sigma^{(3)} \right\} \otimes \boldsymbol{T}_{p_2}(\mathbf{q}, S_\pi) \tag{8}$$

If

$$\boldsymbol{p}_{\mu\mu'}(\mathbf{q}, \lambda, \pi) = \frac{d_\lambda}{h} \sum_{\sigma=1}^{g_{N(p)}} \tau^*_{\mu\mu'}(\mathbf{q}, \lambda, S_{\pi,\sigma})\, \boldsymbol{S}_\sigma^{(3)} \tag{9}$$

then

$$\mathbf{P}_{\mu\mu'}(\mathbf{q}, \lambda, p) = \sum_{\pi=1}^{f} \boldsymbol{p}_{\mu\mu'}(\mathbf{q}, \lambda, \pi) \otimes \boldsymbol{T}_p(\mathbf{q}, S_\pi)$$

and

$$\mathbf{P}_{\mu\mu'}(\mathbf{q}, \lambda) = \mathbf{P}_{\mu\mu'}(\mathbf{q}, \lambda, p_1) \oplus \mathbf{P}_{\mu\mu'}(\mathbf{q}, \lambda, p_2) \tag{10}$$

$T_p\,(q, S_{\pi,\sigma})$ *matrices.*

Since we shall be concerned with symmetry properties of lattice modes for wavevectors

within the Brillouin zone, the phase factor exp $[i\mathbf{G}\cdot\{\boldsymbol{x}(\kappa) - \mathbf{v}(S)\}]$ that appears in $\boldsymbol{T}(\mathbf{q}, S)$ (equation (2)) is unity as $G = 0$ for $\mathbf{q}$ within the Brillouin zone. Hence $\boldsymbol{T}_p(\mathbf{q}, S_{\pi,\sigma})$ matrices are as given in table 6 for Sb_2S_3. In writing these matrices it may again be noted that the 'pseudo-molecular' concept is implied and hence factors $\delta_{ii'}$ $C^i(S)$ do not appear.

3.4 *Projection operators and symmetry vector matrices for specific wavevectors*

We shall now consider four specific wavevectors, namely, $\mathbf{q}_1 = 0$; $\mathbf{q}_2 = (Q_1, 0, 0)$; $\mathbf{q}_3 = (0, Q_2, 0)$ and $\mathbf{q}_4 = (0, 0, Q_3)$. We shall construct projection operators and then derive the symmetry vector matrices for each of these cases. Table 7 provides the

Table 6. $\boldsymbol{T}_1(\mathbf{q}, S_{\pi,\sigma})$ matrices for Sb_2S_3 (pseudomolecular) (q within brillouin zone).

$$\boldsymbol{T}_1(\mathbf{q}, S_{\mathrm{I},1}) = \begin{vmatrix} h_1 & 0 & 0 & 0 \\ 0 & h_1 & 0 & 0 \\ 0 & 0 & h_1 & 0 \\ 0 & 0 & 0 & h_1 \end{vmatrix} \qquad \boldsymbol{T}_1(\mathbf{q}, S_{\mathrm{I},2}) = \begin{vmatrix} h_{27} & 0 & 0 & 0 \\ 0 & h_{27} & 0 & 0 \\ 0 & 0 & h_{27} & 0 \\ 0 & 0 & 0 & h_{27} \end{vmatrix}$$

$$\boldsymbol{T}_1(\mathbf{q}, S_{\mathrm{II},1}) = \begin{vmatrix} 0 & h_2 & 0 & 0 \\ h_2 & 0 & 0 & 0 \\ 0 & 0 & 0 & h_2 \\ 0 & 0 & h_2 & 0 \end{vmatrix} \qquad \boldsymbol{T}_1(\mathbf{q}, S_{\mathrm{II},2}) = \begin{vmatrix} 0 & h_{28} & 0 & 0 \\ h_{28} & 0 & 0 & 0 \\ 0 & 0 & 0 & h_{28} \\ 0 & 0 & h_{28} & 0 \end{vmatrix}$$

$$\boldsymbol{T}_1(\mathbf{q}, S_{\mathrm{III},1}) = \begin{vmatrix} 0 & 0 & h_3 & 0 \\ 0 & 0 & 0 & h_3 \\ h_3 & 0 & 0 & 0 \\ 0 & h_3 & 0 & 0 \end{vmatrix} \qquad \boldsymbol{T}_1(\mathbf{q}, S_{\mathrm{III},2}) = \begin{vmatrix} 0 & 0 & h_{25} & 0 \\ 0 & 0 & 0 & h_{25} \\ h_{25} & 0 & 0 & 0 \\ 0 & h_{25} & 0 & 0 \end{vmatrix}$$

$$\boldsymbol{T}_1(\mathbf{q}, S_{\mathrm{IV},1}) = \begin{vmatrix} 0 & 0 & 0 & h_4 \\ 0 & 0 & h_4 & 0 \\ 0 & h_4 & 0 & 0 \\ h_4 & 0 & 0 & 0 \end{vmatrix} \qquad \boldsymbol{T}_1(\mathbf{q}, S_{\mathrm{IV},2}) = \begin{vmatrix} 0 & 0 & 0 & h_{26} \\ 0 & 0 & h_{26} & 0 \\ 0 & h_{26} & 0 & 0 \\ h_{26} & 0 & 0 & 0 \end{vmatrix}$$

Table 7(a). Irreducible representations for groups of wave-vectors $G_0(\mathbf{q})$

(i) $\mathbf{q} = 0$ $G_0(\mathbf{q})$: $\{h_1, h_2, h_3, h_4, h_{25}, h_{26}, h_{27}, h_{28}\}$.

		h_1	h_2	h_3	h_4	h_{25}	h_{26}	h_{27}	h_{28}	
Γ_1	(A_g)	1	1	1	1	1	1	1	1	α_{xx}, α_{yy}, α_{zz}
Γ_2	(A_u)	1	1	1	1	−1	−1	−1	−1	
Γ_3	(B_{3g})	1	1	−1	−1	1	1	−1	−1	R_x, α_{yz}
Γ_4	(B_{2g})	1	−1	1	−1	1	−1	1	−1	R_y, α_{zx}
Γ_5	(B_{1g})	1	−1	−1	1	1	1	−1	1	R_z, α_{xy}
Γ_6	(B_{3u})	1	1	−1	−1	−1	−1	1	1	T_x
Γ_7	(B_{1u})	1	−1	−1	1	−1	1	1	−1	T_y
Γ_8	(B_{2u})	1	−1	1	−1	−1	1	−1	1	T_z

(ii) $\mathbf{q} = \mathbf{q}_2 = (Q_1, 0, 0)$ $G_0(\mathbf{q}_2)$: $\{h_1, h_2, h_{27}, h_{28}\}$ Σ direction

(iii) $\mathbf{q} = \mathbf{q}_3 = (0, Q_2, 0)$ $G_0(\mathbf{q}_3)$: $\{h_1, h_3, h_{26}, h_{28}\}$ Δ direction

(iv) $\mathbf{q} = \mathbf{q}_4 = (0, 0, Q_3)$ $G_0(\mathbf{q}_4)$: $\{h_1, h_4, h_{26}, h_{27}\}$ Λ direction

Σ_1	Δ_1	Λ_1	1	1	1	1
Σ_2	Δ_2	Λ_2	1	1	−1	−1
Σ_3	Δ_3	Λ_3	1	−1	1	−1
Σ_4	Δ_4	Λ_4	1	−1	−1	1

Table 7(b). Compatibility relations in paraelectric Sb_2S_3.

$10\,\Gamma_1$, $10\,\Gamma_6$	$20\,\Sigma_1$	$10\,\Gamma_1$, $5\,\Gamma_8$	$15\,\Delta_1$	$10\,\Gamma_1$, $10\,\Gamma_7$	$20\,\Lambda_1$
$5\,\Gamma_2$, $5\,\Gamma_3$	$10\,\Sigma_2$	$5\,\Gamma_2$, $10\,\Gamma_4$	$15\,\Delta_2$	$5\,\Gamma_2$, $5\,\Gamma_5$	$10\,\Lambda_2$
$10\,\Gamma_4$, $10\,\Gamma_7$	$20\,\Sigma_3$	$5\,\Gamma_3$, $10\,\Gamma_7$	$15\,\Delta_3$	$5\,\Gamma_3$, $5\,\Gamma_8$	$10\,\Lambda_3$
$5\,\Gamma_5$, $5\,\Gamma_8$	$10\,\Sigma_4$	$5\,\Gamma_5$, $10\,\Gamma_6$	$15\,\Delta_4$	$10\,\Gamma_4$, $10\,\Gamma_6$	$20\,\Lambda_4$

irreducible representations for the groups of the four wavevectors. We note that for Sb_2S_3 since $p_1=0$ and $p_2=1$, $P_{\mu\mu'}(\mathbf{q}, \lambda)=P_{\mu\mu'}(\mathbf{q}, \lambda, p_2=1)$.

$\underline{\mathbf{q}_1=0}$

$$G_0(\mathbf{q}): \{h_1, h_2, h_3, h_4, h_{25}, h_{26}, h_{27} \text{ and } h_{28}\}.$$

Since the irreducible representations are all one-dimensional (*i.e.* $\mu=\mu'=1$) we have to compute $P_{11}(0, \Gamma_n, \pi)$ using eq (9). The result is as given below ($p_2=1$):

Γ_n \ π	$p_{11}(0, \Gamma_n, \pi)$ I	II	III	IV
Γ_1	t_1	t_2	$-t_1$	$-t_2$
Γ_2	t_3	$-t_3$	t_3	$-t_3$
Γ_3	t_3	$-t_3$	$-t_3$	t_3
Γ_4	t_1	$-t_2$	$-t_1$	t_2
Γ_5	t_3	t_3	$-t_3$	$-t_3$
Γ_6	t_1	t_2	t_1	t_2
Γ_7	t_1	$-t_2$	t_1	$-t_2$
Γ_8	t_3	t_3	t_3	t_3

where $t_1 = \frac{1}{2}\begin{vmatrix} 1 & 0 & 0 \\ 0 & 0 & 0 \\ 0 & 0 & 1 \end{vmatrix}$, $t_2 = \frac{1}{2}\begin{vmatrix} 1 & 0 & 0 \\ 0 & 0 & 0 \\ 0 & 0 & -1 \end{vmatrix}$, $t_3 = \frac{1}{2}\begin{vmatrix} 0 & 0 & 0 \\ 0 & 1 & 0 \\ 0 & 0 & 0 \end{vmatrix}$

From (10), we have

$$\boldsymbol{P}_{11}(0, \Gamma_n) = p_{11}(0, \Gamma_n, \mathrm{I})\boldsymbol{T}_1(S_{\mathrm{I}}) + p_{11}(0, \Gamma_n, \mathrm{II})\boldsymbol{T}_1(S_{\mathrm{II}}) + p_{11}(0, \Gamma_n, \mathrm{III})\boldsymbol{T}_1(S_{\mathrm{III}}) + p_{11}(0, \Gamma_n, \mathrm{IV})\boldsymbol{T}_1(S_{\mathrm{IV}}).$$

The projection operators obtained using this expression are given in table 8(a). Once the projection operators are determined it is straightforward to derive the symmetry vectors belonging to different representations. They are the independent vectors obtained by operating the projection operators on the set of basis vectors. Collection of symmetry vectors, representation by representation, provides the symmetry vector matrix needed for block diagonalisation of the dynamical matrix. In the present case, the symmetry vector matrix ξ (0) (derived by inspection) is given by,

$$\xi(0)=\frac{1}{2}\left|\begin{array}{cccccccccccc|c|c}
1&0&0&0&1&0&0&1&0&1&0&0&x\\
0&0&1&1&0&0&1&0&0&0&0&1&y\}1\\
0&1&0&0&0&1&0&0&1&0&1&0&z\\
\hline
1&0&0&0&-1&0&0&1&0&-1&0&0&x\\
0&0&-1&-1&0&0&1&0&0&0&0&1&y\}2\\
0&-1&0&0&0&1&0&0&-1&0&1&0&z\\
\hline
-1&0&0&0&-1&0&0&1&0&1&0&0&x\\
0&0&1&-1&0&0&-1&0&0&0&0&1&y\}3\\
0&-1&0&0&0&-1&0&0&1&0&1&0&z\\
\hline
-1&0&0&0&1&0&0&1&0&-1&0&0&x\\
0&0&-1&1&0&0&-1&0&0&0&0&1&y\}4\\
0&1&0&0&0&-1&0&0&-1&0&1&0&z
\end{array}\right|\otimes 1_5$$

$\underbrace{\quad}_{\Gamma_1}\ \Gamma_2\ \Gamma_3\ \underbrace{\quad}_{\Gamma_4}\ \Gamma_5\ \underbrace{\quad}_{\Gamma_6}\ \underbrace{\quad}_{\Gamma_7}\ \Gamma_8$

Table 8. Projection operators for specific wavevectors.

(a) $P(0, \Gamma_r)$ $r = 1$ through 8.

$$\left|\begin{array}{cccc}t_1&t_2&-t_1&-t_2\\t_2&t_1&-t_2&-t_1\\-t_1&-t_2&t_1&t_2\\-t_2&-t_1&t_2&t_1\end{array}\right|_{\Gamma_1}\quad\left|\begin{array}{cccc}t_3&-t_3&t_3&-t_3\\-t_3&t_3&-t_3&t_3\\t_3&-t_3&t_3&-t_3\\-t_3&t_3&-t_3&t_3\end{array}\right|_{\Gamma_2}\quad\left|\begin{array}{cccc}t_3&-t_3&-t_3&t_3\\-t_3&t_3&t_3&-t_3\\-t_3&t_3&t_3&-t_3\\t_3&-t_3&-t_3&t_3\end{array}\right|_{\Gamma_3}$$

$$\left|\begin{array}{cccc}t_1&-t_2&-t_1&t_2\\-t_2&t_1&t_2&-t_1\\-t_1&t_2&t_1&-t_2\\t_2&-t_1&-t_2&t_1\end{array}\right|_{\Gamma_4}\quad\left|\begin{array}{cccc}t_3&t_3&-t_3&-t_3\\t_3&t_3&-t_3&-t_3\\-t_3&-t_3&t_3&t_3\\-t_3&-t_3&t_3&t_3\end{array}\right|_{\Gamma_5}\quad\left|\begin{array}{cccc}t_1&t_2&t_1&t_2\\t_2&t_1&t_2&t_1\\t_1&t_2&t_1&t_2\\t_2&t_1&t_2&t_1\end{array}\right|_{\Gamma_6}$$

$$\left|\begin{array}{cccc}t_1&-t_2&t_1&-t_2\\-t_2&t_1&-t_2&t_1\\t_1&-t_2&t_1&-t_2\\-t_2&t_1&-t_2&t_1\end{array}\right|_{\Gamma_7}\quad\left|\begin{array}{cccc}t_3&t_3&t_3&t_3\\t_3&t_3&t_3&t_3\\t_3&t_3&t_3&t_3\\t_3&t_3&t_3&t_3\end{array}\right|_{\Gamma_8}$$

(b) $P(\mathbf{q}_2, \Sigma_r)$ $r = 1$ through 4.

$$\left|\begin{array}{cccc}t_1&t_2&0&0\\t_2&t_1&0&0\\0&0&t_1&t_2\\0&0&t_2&t_1\end{array}\right|_{\Sigma_1}\quad\left|\begin{array}{cccc}t_3&-t_3&0&0\\-t_3&t_3&0&0\\0&0&t_3&-t_3\\0&0&-t_3&t_3\end{array}\right|_{\Sigma_2}\quad\left|\begin{array}{cccc}t_1&-t_2&0&0\\-t_2&t_1&0&0\\0&0&t_1&-t_2\\0&0&-t_2&t_1\end{array}\right|_{\Sigma_3}\quad\left|\begin{array}{cccc}t_3&t_3&0&0\\t_3&t_3&0&0\\0&0&t_3&t_3\\0&0&t_3&t_3\end{array}\right|_{\Sigma_4}$$

(c) $P(\mathbf{q}_3, \Delta_r)$ $r = 1$ through 4

$$\left|\begin{array}{cccc}t_1&t_2&t_3&t_4\\t_2&t_1&t_4&t_3\\t_3&t_4&t_1&t_2\\t_4&t_3&t_2&t_1\end{array}\right|_{\Delta_1}\quad\left|\begin{array}{cccc}t_1&-t_2&t_3&-t_4\\-t_2&t_1&-t_4&t_3\\t_3&-t_4&t_1&-t_2\\-t_4&t_3&-t_2&t_1\end{array}\right|_{\Delta_2}\quad\left|\begin{array}{cccc}t_1&-t_2&-t_3&t_4\\-t_2&t_1&t_4&-t_3\\-t_3&t_4&t_1&-t_2\\t_4&-t_3&-t_2&t_1\end{array}\right|_{\Delta_3}\quad\left|\begin{array}{cccc}t_1&t_2&-t_3&-t_4\\t_2&t_1&-t_4&-t_3\\-t_3&-t_4&t_1&t_2\\-t_4&t_3&t_1&t_2\end{array}\right|_{\Delta_4}$$

(d) $P(\mathbf{q}_4, \Lambda_r)$ $r = 1$ through 4

$$\left|\begin{array}{cccc}t_1&0&0&t_2\\0&t_1&t_2&0\\0&t_2&t_1&0\\t_2&0&0&t_1\end{array}\right|_{\Lambda_1}\quad\left|\begin{array}{cccc}t_3&0&0&-t_3\\0&t_3&-t_3&0\\0&-t_3&t_3&0\\-t_3&0&0&t_3\end{array}\right|_{\Lambda_2}\quad\left|\begin{array}{cccc}t_3&0&0&t_3\\0&t_3&t_3&0\\0&t_3&t_3&0\\t_3&0&0&t_3\end{array}\right|_{\Lambda_3}\quad\left|\begin{array}{cccc}t_1&0&0&-t_2\\0&t_1&-t_2&0\\0&-t_2&t_1&0\\-t_2&0&0&t_1\end{array}\right|_{\Lambda_4}$$

The index κ associated with each 'pseudo-molecule' and corresponding displacements x, y and z are indicated. The factor $\otimes \mathbf{1}_5$ indicates that for use in dynamical calculations one can change over to the atomic model by replacing each set of three rows of displacement vectors associated with every representation and every 'pseudo-molecular' index $\kappa(=1, 2, \ldots, n(p_2))$ by a 5×5 dimensional diagonal matrix with the diagonal 'elements' being the corresponding set of three rows of displacement vectors. The enlargement factor five is equal to the number of atoms in the 'pseudo-molecule' Sb_2S_3.

Classification: Using the relation,

$$C_{\tau_i}(\mathbf{q}) = \frac{1}{g} \sum_{S_n} \chi\{\tau_i(\mathbf{q}, S_n)\}\, \chi\{\mathbf{T}(\mathbf{q}, S_n)\};\ S_n \in G_0(\mathbf{q}), \tag{11}$$

the number of times the representation τ_i appears in the $3j$-dimensional space can be derived. We have, the 60 modes at q_1 classified as

$$10\,\Gamma_1 + 5\,\Gamma_2 + 5\,\Gamma_3 + 10\,\Gamma_4 + 5\,\Gamma_5 + 10\,\Gamma_6 + 10\,\Gamma_7 + 5\,\Gamma_8.$$

For the other wavevectors we shall briefly give the results in the following. The procedure is similar to what we have outlined above for $\mathbf{q}_1$.

$\underline{\mathbf{q}_2 = (Q_1, 0, 0)}$

$G_0(\mathbf{q}_1)$: $\{h_1, h_3, h_{27}$ and $h_{28}\}$

π : I II I II

Σ_n \ π	$p_{11}(0, \Sigma, \pi)$ I	II
Σ_1	t_1	t_2
Σ_2	t_3	$-t_3$
Σ_3	t_1	$-t_2$
Σ_4	t_3	t_3

$$t_1 = \begin{vmatrix} 1 & 0 & 0 \\ 0 & 0 & 0 \\ 0 & 0 & 1 \end{vmatrix}, \quad t_2 = \begin{vmatrix} 1 & 0 & 0 \\ 0 & 0 & 0 \\ 0 & 0 & -1 \end{vmatrix} \text{ and } \quad t_3 = \begin{vmatrix} 0 & 0 & 0 \\ 0 & 1 & 0 \\ 0 & 0 & 0 \end{vmatrix}.$$

Projection operators are given in table 8(b). The symmetry vector matrix for the 'pseudo-molecular' Sb_2S_3 is given by,

$$\xi(\mathbf{q}_2) = \frac{1}{\sqrt{2}} \left|\begin{array}{cccccccccccc|cc}
1 & 0 & 0 & 0 & 0 & 0 & 1 & 0 & 0 & 0 & 0 & 0 & x & \kappa \\
0 & 0 & 0 & 0 & 1 & 0 & 0 & 0 & 0 & 0 & 1 & 0 & y & 1 \\
0 & 1 & 0 & 0 & 0 & 0 & 0 & 1 & 0 & 0 & 0 & 0 & z & \\
1 & 0 & 0 & 0 & 0 & 0 & -1 & 0 & 0 & 0 & 0 & 0 & x & \\
0 & 0 & 0 & 0 & -1 & 0 & 0 & 0 & 0 & 0 & 1 & 0 & y & 2 \\
0 & -1 & 0 & 0 & 0 & 0 & 0 & 1 & 0 & 0 & 0 & 0 & z & \\
0 & 0 & 1 & 0 & 0 & 0 & 0 & 0 & 1 & 0 & 0 & 0 & x & \\
0 & 0 & 0 & 0 & 0 & 1 & 0 & 0 & 0 & 0 & 0 & 1 & y & 3 \\
0 & 0 & 0 & 1 & 0 & 0 & 0 & 0 & 0 & 1 & 0 & 0 & z & \\
0 & 0 & 1 & 0 & 0 & 0 & 0 & 0 & -1 & 0 & 0 & 0 & x & \\
0 & 0 & 0 & 0 & 0 & -1 & 0 & 0 & 0 & 0 & 0 & 1 & y & 4 \\
0 & 0 & 0 & -1 & 0 & 0 & 0 & 0 & 0 & 1 & 0 & 0 & z & \\
\underbrace{\qquad\qquad}_{\Sigma_1} & & & & \underbrace{\quad}_{\Sigma_2} & & \underbrace{\qquad\qquad}_{\Sigma_3} & & & & \underbrace{\quad}_{\Sigma_4} & & & \otimes \mathbf{1}_5
\end{array}\right|$$

Classification: $20\ \Sigma_1 + 10\ \Sigma_2 + 20\ \Sigma_3 + 10\ \Sigma_4$. The full symmetry vector matrix is obtained as explained earlier for the case of $\mathbf{q}_1$

$\underline{\mathbf{q}_3 = (0, Q_2, 0)}$

$G_0\ (\mathbf{q}_3)$: $\{h_1, h_3, h_{26}$ and $h_{28}\}$
π : I II III IV

Δ_n \ π	$p_{11}\ (\mathbf{q}_3, \Delta_n, \pi)$ I	II	III	IV
Δ_1	t_1	t_2	t_3	t_4
Δ_2	t_1	$-t_2$	t_3	$-t_4$
Δ_3	t_1	$-t_2$	$-t_3$	t_4
Δ_4	t_1	t_2	$-t_3$	$-t_4$

where $t_1 = \begin{vmatrix} 1 & 0 & 0 \\ 0 & 1 & 0 \\ 0 & 0 & 1 \end{vmatrix}$, $t_2 = \begin{vmatrix} 1 & 0 & 0 \\ 0 & 1 & 0 \\ 0 & 0 & -1 \end{vmatrix}$, $t_3 = \begin{vmatrix} -1 & 0 & 0 \\ 0 & 1 & 0 \\ 0 & 0 & -1 \end{vmatrix}$ and $t_4 = \begin{vmatrix} -1 & 0 & 0 \\ 0 & 1 & 0 \\ 0 & 0 & 1 \end{vmatrix}$

Projection operators are given in table 8(c). The symmetry vector matrix for $\mathbf{q}_3$ is given by,

$$\xi\ (\mathbf{q}_3) = \tfrac{1}{2} \left| \begin{array}{cccccccccccc|c|c} 1 & 0 & 0 & 1 & 0 & 0 & 1 & 0 & 0 & 1 & 0 & 0 & x & \kappa \\ 0 & 1 & 0 & 0 & 1 & 0 & 0 & 1 & 0 & 0 & 1 & 0 & y & 1 \\ 0 & 0 & 1 & 0 & 0 & 1 & 0 & 0 & 1 & 0 & 0 & 1 & z & \\ \hline 1 & 0 & 0 & -1 & 0 & 0 & -1 & 0 & 0 & 1 & 0 & 0 & x & \\ 0 & 1 & 0 & 0 & -1 & 0 & 0 & -1 & 0 & 0 & 1 & 0 & y & 2 \\ 0 & 0 & -1 & 0 & 0 & 1 & 0 & 0 & 1 & 0 & 0 & -1 & z & \\ \hline -1 & 0 & 0 & -1 & 0 & 0 & 1 & 0 & 0 & 1 & 0 & 0 & x & \\ 0 & 1 & 0 & 0 & 1 & 0 & 0 & -1 & 0 & 0 & -1 & 0 & y & 3 \\ 0 & 0 & -1 & 0 & 0 & -1 & 0 & 0 & 1 & 0 & 0 & 1 & z & \\ \hline -1 & 0 & 0 & 1 & 0 & 0 & -1 & 0 & 0 & 1 & 0 & 0 & x & \\ 0 & 1 & 0 & 0 & -1 & 0 & 0 & 1 & 0 & 0 & -1 & 0 & y & 4 \\ 0 & 0 & 1 & 0 & 0 & -1 & 0 & 0 & 1 & 0 & 0 & -1 & z & \\ \hline \multicolumn{3}{c}{\Delta_1} & \multicolumn{3}{c}{\Delta_2} & \multicolumn{3}{c}{\Delta_3} & \multicolumn{3}{c}{\Delta_4} & & \end{array} \right| \otimes \mathbf{1}_5$$

Classification: $15\ \Delta_1 + 15\ \Delta_2 + 15\ \Delta_3 + 15\ \Delta_4$

$\underline{\mathbf{q}_4 = (0, 0, Q_3)}$

$G_0\ (\mathbf{q}_4)$: h_1, h_4, h_{26} and h_{27}
π : I IV IV I

Λ_n/π	$p_{11}\ (\mathbf{q}_4, \Lambda_n, \pi)$ I	IV
Λ_1	t_1	t_2
Λ_2	t_3	$-t_3$
Λ_3	t_3	t_3
Λ_4	t_1	$-t_3$

where $t_1 = \begin{vmatrix} 1 & 0 & 0 \\ 0 & 0 & 0 \\ 0 & 0 & 1 \end{vmatrix}$ $t_2 = \begin{vmatrix} -1 & 0 & 0 \\ 0 & 0 & 0 \\ 0 & 0 & 1 \end{vmatrix}$ and $t_3 = \begin{vmatrix} 0 & 0 & 0 \\ 0 & 1 & 0 \\ 0 & 0 & 1 \end{vmatrix}$

Projection operators are given in table 8(d). The symmetry vector matrix for $\mathbf{q}_4$ is given by

$$\xi(\mathbf{q}_4) = \frac{1}{\sqrt{2}} \left|\begin{array}{cccccccccccc}
1 & 0 & 0 & 0 & 0 & 0 & 0 & 0 & 1 & 0 & 0 & 0 \\
0 & 0 & 0 & 0 & 1 & 0 & 1 & 0 & 0 & 0 & 0 & 0 \\
0 & 1 & 0 & 0 & 0 & 0 & 0 & 0 & 0 & 1 & 0 & 0 \\
0 & 0 & 1 & 0 & 0 & 0 & 0 & 0 & 0 & 0 & 1 & 0 \\
0 & 0 & 0 & 0 & 0 & 1 & 0 & 1 & 0 & 0 & 0 & 0 \\
0 & 0 & 0 & 1 & 0 & 0 & 0 & 0 & 0 & 0 & 0 & 1 \\
0 & 0 & -1 & 0 & 0 & 0 & 0 & 0 & 0 & 0 & 1 & 0 \\
0 & 0 & 0 & 0 & 0 & -1 & 0 & 1 & 0 & 0 & 0 & 0 \\
0 & 0 & 0 & 1 & 0 & 0 & 0 & 0 & 0 & 0 & 0 & -1 \\
-1 & 0 & 0 & 0 & 0 & 0 & 0 & 0 & 1 & 0 & 0 & 0 \\
0 & 0 & 0 & 0 & -1 & 0 & 1 & 0 & 0 & 0 & 0 & 0 \\
0 & 1 & 0 & 0 & 0 & 0 & 0 & 0 & 0 & -1 & 0 & 0
\end{array}\right| \begin{array}{c} \kappa \\ x \\ y \\ z \\ x \\ y \\ z \\ x \\ y \\ z \\ x \\ y \\ z \end{array} \begin{array}{l} \\ \} 1 \\ \\ \\ \} 2 \\ \\ \\ \} 3 \\ \\ \} 4 \\ \\ \end{array} \otimes \mathbf{1}_5$$

$$\underbrace{\qquad}_{\Lambda_1} \quad \underbrace{\quad}_{\Lambda_2} \quad \underbrace{\quad}_{\Lambda_4} \quad \underbrace{\qquad}_{\Lambda_3}$$

Classification: $20\,\Lambda_1 + 10\,\Lambda_2 + 10\,\Lambda_3 + 20\,\Lambda_4$

3.5 *Reduction of dynamical matrix*

The dynamical matrix $\mathbf{M}(\mathbf{q})$ defined by (Rao *et al* 1978)

$$M_{\alpha\beta}^{ii'}\begin{pmatrix}\mathbf{q}\\ \kappa\kappa'\end{pmatrix} = \sum_{l'} \Phi^{ii'}\begin{pmatrix}0 & l'\\ \kappa & \kappa'\end{pmatrix} \exp\left\{i\mathbf{q}.\mathbf{x}\begin{pmatrix}0 & l'\\ \kappa & \kappa'\end{pmatrix}\right\} \tag{12}$$

commutes with $\boldsymbol{T}(\mathbf{q}, S)$ defined by (2) for all $S \in G_0(\mathbf{q})$. Since we shall be interested in an atomic model of lattice dynamics in Sb_2S_3, we shall restrict i and i' to translation only and with this understanding drop the superscripts ii' in the following. $\boldsymbol{T}(\mathbf{q}, S)$ (Eq. 2) reduces to

$$T_{\alpha\beta}(\mathbf{q}, \kappa\kappa', S) = S_{\alpha\beta}\,\delta[\kappa, F_0(\kappa', S)] \exp\left[i\mathbf{G}\cdot\{\mathbf{x}(\kappa) - \mathbf{v}(S)\}\right]$$

$$= S_{\alpha\beta}\,\delta[\kappa, F_0(\kappa', S)], \tag{13}$$

for $\mathbf{q}$ within the Brillouin zone. The commutation relation is,

$$\boldsymbol{T}(\mathbf{q}, S)\,\boldsymbol{M}(\mathbf{q}) = \boldsymbol{M}(\mathbf{q})\,\boldsymbol{T}(\mathbf{q}, S),$$

i.e.
$$[\boldsymbol{S}^{(3)} \otimes \boldsymbol{T}^J(\mathbf{q}, S)]\,\boldsymbol{M}(\mathbf{q}) = \boldsymbol{M}(\mathbf{q})\,[\boldsymbol{S}^{(3)} \otimes \boldsymbol{T}^J(\mathbf{q}, S)]. \tag{14}$$

These relations help to reduce the dynamical matrix. The procedure outlined by Sieskind is quite elegant and useful and we have followed this approach. Sieskind (1978) considers the general element of $\boldsymbol{T}^J(\mathbf{q}, S)$ which is independent of $\alpha, \beta = 1, 2, 3$ and specialising to the case where there is one and only one non-zero element in each row and column in $\boldsymbol{S}^{(3)}$ matrices (as it happens in D_{2h}^{16}), we have,

$$\sum_{\gamma=1}^{3}\sum_{\kappa=1}^{j} S^{(3)}_{\alpha\gamma}\, T^{J}(K\kappa, \mathbf{q}, S)\, M_{\gamma\beta}(\kappa K', \mathbf{q}) = \sum_{\nu=1}^{3}\sum_{\kappa'=1}^{j} M_{\alpha\nu}(K\kappa', \mathbf{q})\, T^{J}(\kappa' K', \mathbf{q}, S)\, S^{(3)}_{\nu\beta}$$

or

$$\sum_{\kappa=1}^{j} T^{J}(K\kappa, \mathbf{q}, S) \sum_{\gamma=1}^{3} S^{(3)}_{\alpha\gamma}\, M_{\gamma\beta}(\kappa K', \mathbf{q}) = \sum_{\kappa'=1}^{j} T^{J}(\kappa' K', \mathbf{q}, S) \sum_{\nu=1}^{3} M_{\alpha\nu}(K\kappa', \mathbf{q})\, S^{(3)}_{\nu\beta}$$

or

$$\sum_{\kappa=1}^{j} T^{J}(K\kappa, \mathbf{q}, S)\, S^{(3)}_{\alpha\zeta}\, M_{\zeta\beta}(\kappa K', \mathbf{q}) = \sum_{\kappa'=1}^{j} M_{\alpha\theta}(K\kappa', \mathbf{q})\, S^{(3)}_{\theta\beta}\, T^{J}(\kappa' K', \mathbf{q}, S) \qquad (15)$$

where ζ, θ are characterised by α, β and S but are independent of K, K', κ, κ' and $S^{(3)}_{\alpha\beta} = \pm 1$. With respect to $\boldsymbol{T}^{J}(\mathbf{q}, S)$ it is convenient to consider the matrix with nine elements $M_{\alpha\beta}(K\kappa', \mathbf{q})$ ($\alpha, \beta = 1, 2, 3$ and $K, \kappa', \mathbf{q}$ fixed) as the entity $M'(K\kappa', \mathbf{q})$ independent of α and β and its corresponding matrix $\boldsymbol{M}'(\mathbf{q})$. Consequently, eliminating the factor $S^{(3)}_{\alpha\beta}$, equation (15) may be written as,

$$\sum_{\kappa=1}^{j} T^{J}(K\kappa, \mathbf{q}, S)\, M'(\kappa K', \mathbf{q}) = \sum_{\kappa'=1}^{j} M'(K\kappa', \mathbf{q})\, T^{J}(\kappa' K', \mathbf{q}, S),$$

or
$$\boldsymbol{T}^{J}(\mathbf{q}, S)\, \boldsymbol{M}'(\mathbf{q}) = \boldsymbol{M}'(\mathbf{q})\, \boldsymbol{T}^{J}(\mathbf{q}, S). \qquad (16)$$

Therefore Sieskind (1978) points out that the reduction of $\boldsymbol{M}(\mathbf{q})$ separates into three separate steps: effects of $\boldsymbol{T}_p(\mathbf{q}, S)$, class effects and effects of $\boldsymbol{S}^{(3)}$

(i) *Effects of* $\mathbf{T}_p(q, S)$ *on* $\mathbf{M}'(K\kappa', q)$

Let us recall that $\boldsymbol{T}^{J}(\mathbf{q}, S)$ is a block diagonal matrix which can be written as a direct sum of $n(p)$-dimensional square matrices $\boldsymbol{T}_p(q, S)$. For the 'pseudomolecular' Sb_2S_3,

$$\boldsymbol{T}^{J}(\mathbf{q}, S) = \boldsymbol{T}_{p_2}(\mathbf{q}, S) \text{ where } p_2 = 1 \text{ and } n(p_2) = 4.$$

In the latter case, $\boldsymbol{M}'(\mathbf{q}) = \boldsymbol{M}'_{11}(\mathbf{q})$ of size 4×4.
Hence, we have

$$\boldsymbol{T}_1(\mathbf{q}, S)\, \boldsymbol{M}'(\mathbf{q}) = \boldsymbol{M}'(\mathbf{q})\, \boldsymbol{T}_1(\mathbf{q}, S), \qquad (17)$$

Where we have dropped the subscript 11 on M'.

(ii) *Class effects*

In case of Sb_2S_3, the four-dimensional permutation matrices $T_1(S_{\pi,\tau})$ arrange them-

selves in four classes $\pi = \text{I, II, III and IV}$. We shall examine the consequences of using the relation (17), namely,

$$\boldsymbol{T}_1(\mathbf{q}, S_{\pi,\sigma})\,\boldsymbol{M}'(\mathbf{q}) = \boldsymbol{M}'(\mathbf{q})\,\boldsymbol{T}_1(\mathbf{q}, S_{\pi,\sigma}),$$

or since the relation is independent of $\mathbf{q}$ and σ, one can write,

$$\boldsymbol{T}_1(S_\pi)\begin{vmatrix} M'(11) & M'(12) & .. & .. \\ M'(21) & .. & .. & .. \\ .. & M'(LL') & & .. \\ .. & .. & .. & .. \end{vmatrix} = \begin{vmatrix} M'(11) & .. & .. & .. \\ .. & .. & .. & .. \\ .. & M'(LL') & .. & \\ .. & .. & .. & .. \end{vmatrix} \boldsymbol{T}_1(S_\pi).$$

Using $\boldsymbol{T}_1(S_{\pi,\sigma})$ given in table 5, we get several relations; for example, considering $\pi = 3$, we have,

$$M'(33) = M'(11);\ M'(34) = M'(12);\ M'(31) = M'(13);\ M'(32) = M'(14), \text{ etc.}$$

Such relations indicate that the 3×3 matrices associated with the pair LL', say, are related to the 3×3 matrices associated with the pair MM', say, as given by these relations. How they will be related will be clear only by considering the effect of $S^{(3)}$.

(iii) *Effect of* $S^{(3)}$

The last step in reduction of the dynamical matrix $\boldsymbol{M}(\mathbf{q})$ takes into consideration effects of $S^{(3)}$ on $\boldsymbol{M}(\mathbf{q})$. Successive applications of the point group operations to the relations obtained by class effects by means of the following relation,

$$\sum_{\gamma=1}^{3} S^{(3)}_{\alpha\gamma}\, M_{\gamma\beta}(LL', \mathbf{q}) = \sum_{\nu=1}^{3} M_{\alpha\nu}(MM', \mathbf{q})\, S^{(3)}_{\nu\beta} \tag{18}$$

would help reduce $\boldsymbol{M}(\mathbf{q})$ further. Note that in this equation, we do not have phase factors as in the case of Sieskind (1978), since $\boldsymbol{T}(\mathbf{q}, S)$ matrices that commute with our dynamical matrix will not have phase factors within the Brillouin zone. We have summarised in table 9 results obtained for 'pseudo-molecular' Sb_2S_3 by combining class effects and effects of $S^{(3)}$.

(iv) *Effects of antiunitary operators*

Sieskind (1978) has not explicitly considered effect of time reversal symmetry which will help further in reduction of dynamical matrix through the use of antiunitary operators. We note that since these are operations $S_- \in G_0$ such that $S_-\mathbf{q} = -\mathbf{q} + \mathbf{G}$, one can use the relation,

$$\boldsymbol{T}(\mathbf{q}, S_-)\,\boldsymbol{M}(\mathbf{q})\,\boldsymbol{T}^{\dagger}(\mathbf{q}, S_-) = \boldsymbol{M}^*(\mathbf{q}) \text{ (eq. 19 j of I)} \tag{19}$$

to examine the reduction of dynamical matrix further. $\boldsymbol{T}(\mathbf{q}, S_-)$ is defined by the elements,

$$T_{\alpha\beta}(\kappa\,\kappa', \mathbf{q}, S_-) = \delta_{ii'}\, C^i\,(S_-)\, S_{-\alpha\beta}\, \delta\,[\kappa, F_0(\kappa', S_-)]$$
$$\times \exp\,[i\,\mathbf{G}\cdot\{\mathbf{x}(\kappa) - \mathbf{v}(S)\}]. \tag{20}$$

For $\mathbf{q}$ within the Brillouin zone ($\mathbf{G} = 0$) and specialising to the case of translations only, we have,

$$T_{\alpha\beta}(\kappa\,\kappa', \mathbf{q}, S_-) = S_{-\alpha\beta}\, \delta\,[\kappa, F_0(\kappa', S_-)], \tag{21}$$

anologous to (13) for unitary operators. Use of antiunitary operators can be included in the analysis by making use of table 9 itself. The only point to note is that the class effects involve complex conjugation of $\boldsymbol{M}(\mathbf{q})$ on one side of the relations as indicated in (19).

(v) *Dynamical matrix elements associated with equivalent and non-equivalent atom pairs*

In order to go over to the atomic model from the 'pseudomolecular' model, the prescription to be followed (to determine the dynamical matrix) is that $\boldsymbol{M}(LL')$ is to be replaced by the matrix,

$$\begin{vmatrix} \boldsymbol{M}\begin{pmatrix} LL' \\ 11 \end{pmatrix} \boldsymbol{M}\begin{pmatrix} LL' \\ 12 \end{pmatrix} & \cdots & \boldsymbol{M}\begin{pmatrix} LL' \\ pq \end{pmatrix} \\ \vdots & & \\ \boldsymbol{M}\begin{pmatrix} LL' \\ p\,1 \end{pmatrix} & \cdots & \boldsymbol{M}\begin{pmatrix} LL' \\ pq \end{pmatrix} \end{vmatrix},$$

where p and q run over the number of types of atoms in the 'pseudo-molecules' L and L'. Each of the matrices $\boldsymbol{M}\begin{pmatrix} LL' \\ pq \end{pmatrix}$ are of order 3×3, the structure of which can be determined as follows. We can classify the dynamical matrix elements pertaining to the atom pairs $\begin{pmatrix} LL' \\ pq \end{pmatrix}$ into two types (a) elements that relate 'equivalent' atoms, that is with indices $p = q$ but $L \neq L'$ and (b) elements that relate 'non- equivalent' atoms that is, with $p \neq q$, but $L = L'$ or $L \neq L'$. Then the structure of the matrix $\boldsymbol{M}\begin{pmatrix} LL' \\ pq \end{pmatrix}$ is obtained by using table 9 as follows: Using the indices LL', we can use the appropriate relations that are given in table 9 for GNES elements that occur in $G_0(\mathbf{q})$ or $G_0(-\mathbf{q})$ (that is through class I). In case of equivalent atoms pairs, in addition, the Hermitian nature of dynamical matrix helps in further reduction. In order to exploit this property one can use the remaining class relations that link, say $1L'$ to $L'1$, through unitary or antiunitary operations. Such relations are underlined in table 9. Similar reduction *via* Hermitian property of dynamical matrices is not

Table 9. Combined effects of class effects and $S^{(s)}$ on $M(q)$

Class	Relations due to class effects	Effect of $S^{(s)}$ $\sigma = 1$ $S(\pi, 1)\, M(ll') = M(mm')\, S(\pi, 1)$	$\sigma = 2$ $S(\pi, 2)\, M(ll') = M(mm')\, S(\pi, 2)$
I	$M(ll') = M(ll')$ for any ll'	$M(ll') = \begin{vmatrix} M_{11} & M_{12} & M_{13} \\ M_{21} & M_{22} & M_{23} \\ M_{31} & M_{32} & M_{33} \end{vmatrix}_{ll'}$ $M(ll') = \begin{vmatrix} M_{11} & 0 & M_{13} \\ 0 & M_{22} & 0 \\ M_{31} & 0 & M_{33} \end{vmatrix}_{ll'}$ if h_{π} is unitary operator	$M(ll') = \begin{vmatrix} M_{11}^R & M_{12}^I & M_{13}^R \\ M_{21}^I & M_{22}^R & M_{23}^I \\ M_{31}^R & M_{32}^I & M_{33}^R \end{vmatrix}_{ll'}$ if h_{π} is antiunitary operator
II	$M(21) = M(12)$; $M(41) = M(32)$ $M(22) = M(11)$; $M(42) = M(31)$ $M(23) = M(14)$; $M(43) = M(34)$ $M(24) = M(13)$; $M(44) = M(33)$	$M(ll') = \begin{vmatrix} M_{11} & -M_{12} & -M_{13} \\ -M_{21} & M_{22} & M_{23} \\ -M_{31} & M_{32} & M_{33} \end{vmatrix}_{mm'}$	$M(ll') = \begin{vmatrix} M_{11} & M_{12} & -M_{13} \\ M_{21} & M_{22} & -M_{23} \\ -M_{31} & -M_{32} & M_{33} \end{vmatrix}_{mm'}$
III	$M(31) = M(13)$; $M(41) = M(23)$ $M(32) = M(14)$; $M(42) = M(24)$ $M(33) = M(11)$; $M(43) = M(21)$ $M(34) = M(12)$; $M(44) = M(22)$	$M(ll') = \begin{vmatrix} M_{11} & -M_{12} & M_{13} \\ -M_{21} & M_{22} & -M_{23} \\ M_{31} & -M_{32} & M_{33} \end{vmatrix}_{mm'}$	$M(ll') = \begin{vmatrix} M_{11} & M_{12} & M_{13} \\ M_{21} & M_{22} & M_{23} \\ M_{31} & M_{32} & M_{33} \end{vmatrix}_{mm'}$
IV	$M(41) = M(14)$; $M(31) = M(24)$ $M(42) = M(13)$; $M(32) = M(23)$ $M(43) = M(12)$; $M(33) = M(22)$ $M(44) = M(11)$; $M(34) = M(21)$	$M(ll') = \begin{vmatrix} M_{11} & M_{12} & -M_{13} \\ M_{21} & M_{22} & -M_{23} \\ -M_{31} & -M_{32} & M_{33} \end{vmatrix}_{mm'}$	$M(ll') = \begin{vmatrix} M_{11} & -M_{12} & -M_{13} \\ -M_{21} & M_{22} & M_{23} \\ -M_{31} & M_{32} & M_{33} \end{vmatrix}_{mm'}$

applicable to non-equivalent atom-pairs. In order to write down the entire dynamical matrix, one may use the remaining class relations given in table 9.

3.6 *Structure of dynamical matrix corresponding to specific wavevectors*

(i) $\mathbf{q}_1 = 0 \quad G_0(\mathbf{q}_1)$: $\{h_1, h_2, h_3, h_4, h_{25}, h_{26}, h_{27}, h_{28}\}$

Note that the GNES $h_{27} \in G_0(\mathbf{q}_1)$. Since $\mathbf{q}_1 = 0$, all elements $M_{\alpha\beta}\begin{pmatrix} LL' \\ kk' \end{pmatrix}$ are real; the form of $M\begin{pmatrix} LL' \\ kk' \end{pmatrix}$ due to the GNES h_{27} is

$$M\begin{pmatrix} LL' \\ kk' \end{pmatrix} = \begin{vmatrix} M_{11}^R & 0 & M_{13}^R \\ 0 & M_{22}^R & 0 \\ M_{31}^R & 0 & M_{33}^R \end{vmatrix} \begin{pmatrix} LL' \\ kk' \end{pmatrix},$$

for any $\begin{pmatrix} LL' \\ kk' \end{pmatrix}_0$ Hermitian nature of $\mathbf{M}(\mathbf{q})$ leads to the additional relation.

$$M_{31}\begin{pmatrix} LL' \\ kk \end{pmatrix} = M_{13}\begin{pmatrix} LL' \\ kk \end{pmatrix}$$

for equivalent atom-pairs.

So, the form of $\mathbf{M}\begin{pmatrix} LL' \\ kk' \end{pmatrix}$ matrices for equivalent and nonequivalent atom pairs are given by,

$$\begin{vmatrix} M_{11}^R & 0 & M_{13}^R \\ 0 & M_{22}^R & 0 \\ M_{13}^R & 0 & M_{33}^R \end{vmatrix} \begin{pmatrix} LL' \\ kk \end{pmatrix} \quad \text{and} \quad \begin{vmatrix} M_{11}^R & 0 & M_{13}^R \\ 0 & M_{22}^R & 0 \\ M_{31}^R & 0 & M_{33}^R \end{vmatrix} \begin{pmatrix} LL' \\ kk' \end{pmatrix}$$

respectively, containing 4 and 5 independent elements each. The superscripts R or I in $M_{\alpha\beta}^{R/I}$ indicate that the element $M_{\alpha\beta}$ is purely real or purely imaginary.

(ii) $\mathbf{q}_2 = (Q_1, 0, 0) \qquad G_0(q_2)$: $\{h_1, h_2, h_{27}, h_{28}\}$

Elements in $G_0(\mathbf{q}_2)$ belong to classes I and II only and the GNES h_{27} is a unitary operator. The form of $M\begin{pmatrix} LL' \\ kk' \end{pmatrix}$ due to the GNES is

$$\mathbf{M}\begin{pmatrix} LL' \\ kk' \end{pmatrix} = \begin{vmatrix} M_{11} & 0 & M_{13} \\ 0 & M_{22} & 0 \\ M_{31} & 0 & M_{33} \end{vmatrix} \begin{pmatrix} LL' \\ kk' \end{pmatrix}$$

for equivalent and nonequivalent atom-pairs.
Because of the class relations the equivalent atom-pairs get related to each other. There are two types of relations.

1. $\boldsymbol{M}\begin{pmatrix}LL'\\kk\end{pmatrix}$ related to $\boldsymbol{M}\begin{pmatrix}L'L\\kk\end{pmatrix}$ under unitary operations which get simplified further due to Hermitian nature of $\boldsymbol{M}(\mathbf{q})$.
Specifically,

$$\boldsymbol{M}\begin{pmatrix}11\\kk\end{pmatrix}=\begin{vmatrix} M_{11}^R & 0 & M_{13} \\ 0 & M_{22}^R & 0 \\ M_{13}^* & 0 & M_{33}^R \end{vmatrix}\begin{pmatrix}11\\kk\end{pmatrix}$$

and

$$\boldsymbol{M}\begin{pmatrix}22\\kk\end{pmatrix}=\begin{vmatrix} M_{11}^R & 0 & -M_{13} \\ 0 & M_{22}^R & 0 \\ M_{13}^* & 0 & M_{33}^R \end{vmatrix}\begin{pmatrix}11\\kk\end{pmatrix}$$

each having 5 independent elements.

2. $\boldsymbol{M}\begin{pmatrix}LL'\\kk\end{pmatrix}$ related to $M\begin{pmatrix}L''L'''\\kk\end{pmatrix}$ under unitary operations: Hermitian property cannot be invoked. Example $\boldsymbol{M}\begin{pmatrix}23\\kk\end{pmatrix}=\boldsymbol{M}\begin{pmatrix}14\\kk\end{pmatrix}$ under class II operations but they are not related to each other through Hermitian relation. However, in these cases, antiunitary operators help to simplify the form of $\boldsymbol{M}\begin{pmatrix}LL'\\kk\end{pmatrix}$ since Hermitian property can be invoked over these antiunitary class relations. As an example we note that $\boldsymbol{M}\begin{pmatrix}41\\kk\end{pmatrix}$ and $\boldsymbol{M}\begin{pmatrix}14\\kk\end{pmatrix}$ are related to each other through an antiunitary operation in class IV. This relation is governed by the Hermitian relation also.
Explicitly,

$$\boldsymbol{M}\begin{pmatrix}41\\kk\end{pmatrix}=\begin{vmatrix} M_{11} & 0 & -M_{13} \\ 0 & M_{22} & 0 \\ -M_{31} & 0 & M_{33} \end{vmatrix}^*\begin{pmatrix}14\\kk\end{pmatrix}$$

through antiunitary class relation and

$$\boldsymbol{M}\begin{pmatrix}41\\kk\end{pmatrix}=\begin{vmatrix} M_{11} & 0 & M_{31} \\ 0 & M_{22} & 0 \\ M_{13} & 0 & M_{33} \end{vmatrix}^*\begin{pmatrix}14\\kk\end{pmatrix}$$

through Hermitian relation. Hence finally we have

$$\mathbf{M}\begin{pmatrix}41\\kk\end{pmatrix}=\begin{vmatrix} M_{11} & 0 & -M_{13}\\ 0 & M_{22} & 0\\ +M_{13} & 0 & M_{33}\end{vmatrix}^{*}\begin{pmatrix}14\\kk\end{pmatrix}$$

$\mathbf{M}\begin{pmatrix}14\\kk\end{pmatrix}$ is therefore of the form

$$\begin{vmatrix} M_{11} & 0 & M_{13}\\ 0 & M_{22} & 0\\ -M_{13} & 0 & M_{33}\end{vmatrix}$$

having 8 independent elements. Similar simplifications can be visualised for other atom-pairs.

For nonequivalent pairs, no further reduction beyond what is given by GNES h_{27} is possible and hence each $M\begin{pmatrix}LL'\\kk'\end{pmatrix}$ will have 10 independent elements.

(iii) $\mathbf{q}_3=(0, Q_3, 0)$ $\qquad G_0(\mathbf{q}_3)$: $\{h_1, h_3, h_{26}, h_{28}\}$

We note that the GNES h_{27} is an antiunitary operator in this case. Hence,

$$M\begin{pmatrix}LL'\\kk'\end{pmatrix}=\begin{vmatrix} M_{11}^{R} & M_{12}^{I} & M_{13}^{R}\\ M_{21}^{I} & M_{22}^{R} & M_{23}^{I}\\ M_{31}^{R} & M_{32}^{I} & M_{33}^{R}\end{vmatrix}\begin{pmatrix}LL'\\kk'\end{pmatrix}$$

for any $\begin{pmatrix}LL'\\kk'\end{pmatrix}$. The classes I, II, III and IV relate the equivalent atom-pairs. Combined with the Hermitian property, $\mathbf{M}\begin{pmatrix}LL'\\kk\end{pmatrix}$ is given by.

$$\mathbf{M}\begin{pmatrix}LL'\\kk\end{pmatrix}=\begin{vmatrix} M_{11}^{R} & M_{12}^{I} & M_{13}^{R}\\ \pm M_{12}^{I} & M_{22}^{R} & M_{23}^{I}\\ \pm M_{13}^{R} & \pm M_{23}^{I} & M_{33}^{R}\end{vmatrix}\begin{pmatrix}LL'\\kk\end{pmatrix}$$

with 6 independent elements. ($\pm$ signs depend on class relations). No further reduction is possible for non-equivalent atom-pairs and each $M\begin{pmatrix}LL'\\kk'\end{pmatrix}$ will have 9 independent elements.

(iv) $\mathbf{q}_4 = (0, 0, Q_3)$ $\quad G_0(\mathbf{q}_4); \{h_1, h_4, h_{26}, h_{27}\}$

Because of the GNES h_{27} being a unitary operator,

$$\boldsymbol{M}\begin{pmatrix} LL' \\ kk' \end{pmatrix} = \begin{vmatrix} M_{11} & 0 & M_{13} \\ 0 & M_{22} & 0 \\ M_{31} & 0 & M_{33} \end{vmatrix} \begin{pmatrix} LL' \\ kk' \end{pmatrix}$$

for any $\begin{pmatrix} LL' \\ kk' \end{pmatrix}$.

Classes I and IV are allowed with unitary operators. Hence as in case of (ii), $\boldsymbol{M}\begin{pmatrix} 14 \\ kk \end{pmatrix}$ and $\boldsymbol{M}\begin{pmatrix} 11 \\ kk \end{pmatrix}$ have the form

$$\begin{vmatrix} M_{11}^R & 0 & M_{13} \\ 0 & M_{22}^R & 0 \\ \pm M_{13}^* & 0 & M_{33}^R \end{vmatrix} \begin{pmatrix} LL' \\ kk \end{pmatrix}$$

and have 5 independent elements each. Others not related by Hermitian property in Class IV but through antiunitary operators will have the structure

$$\begin{vmatrix} M_{11} & 0 & M_{13} \\ 0 & M_{22} & 0 \\ M_{13} & 0 & M_{33} \end{vmatrix}^*$$

and will have 8 independent elements each.
The nonequivalent atom pair matrices will have no further reduction than what is already provided by h_{27} and will have 10 independent elements each.

3.7 *Number of independent elements in M(q)*

According to Casella (1975), excluding accidental degeneracies, if there is no additional degeneracy due to time reversal symmetry, the number of independent elements in $\boldsymbol{M}(\mathbf{q})$ is $\sum_r n_r^2$ where n_r is the number of times the rth irreducible multiplier representation appears in $\boldsymbol{M}(\mathbf{q})$. (Note that $n_r = C_{\tau_i}$ of (11)). But if there is additional degeneracy due to time reversal symmetry, the number of elements can be $\leqslant \sum_r n_r^2$. To check effect of time reversal symmetry, the following procedure is adopted:
(i) Check if $-\mathbf{q}$ is in the star of $\mathbf{q}$, that is, there exists 'connecting operator' S_- in G such that $\boldsymbol{S}_-\mathbf{q} = -\mathbf{q} + \mathbf{G}$. If $-\mathbf{q}$ is not in the star of $\mathbf{q}$, number of independent

elements is given by $N_{\mathrm{I}} = \sum_r n_r^2$ (ii) If $-\mathbf{q}$ is in star of $\mathbf{q}$, the number of elements is given by,

$$N_{\mathrm{II}} = \sum_{r\in a} \tfrac{1}{2} n_r (n_r + 1) + \sum_{r\in b} \tfrac{1}{2} n_r^2 + \sum_{r\in c} \tfrac{1}{2} n_r (n_r - 1) \tag{22}$$

where a, b and c refer to Wigner-Herring time reversal test,

$$\sum_a \exp\{-i(S^{-1}\mathbf{q} + \mathbf{q})\cdot \mathbf{v}(S)\}\chi_r(S^2) = \begin{cases} g_q & \text{case a} \\ 0 & \text{case b} \\ -g_q & \text{case c} \end{cases} \tag{23}$$

Specific cases

For counting the number of independent elements using the knowledge of the structure of dynamical matrix itself, we note that the structure of any $M(LL')$ for Sb_2S_3 is given by,

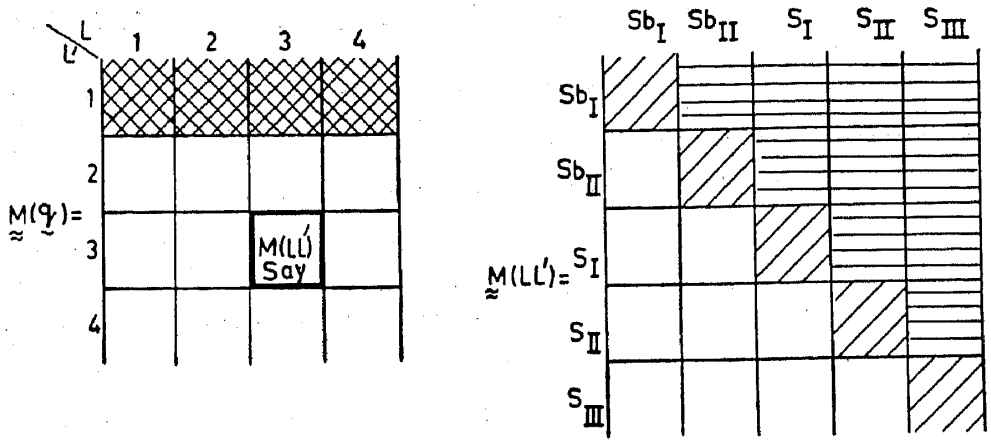

this being one of the 4×4 blocks of the 'pseudomolecular' dynamical matrix $\mathbf{M}(\mathbf{q})$ shown on the left side. In the pseudomolecular scheme, four blocks, say the ones that belong to the first row shown cross hatched (in $\mathbf{M}(\mathbf{q})$), are independent and the other blocks are related to these through class relations. At the atomic level each of the four molecule-molecule blocks consist of five independent equivalent atom-pair blocks along the diagonal shown diagonally hatched and ten independent non-equivalent atom pair blocks shown horizontally hatched. The latter are related to remaining blocks. Hence $N[\mathbf{M}(\mathbf{q})]$ the number of independent elements in the atomic model of dynamics is given by,

$$N[\mathbf{M}(\mathbf{q})] = \left\{\begin{array}{l} \text{(number of equivalent atom-pair blocks in one molecule-pair block) namely 5} \times \text{(Sum of number of independent elements in each of the equivalent atom-pair blocks one per LL' of the first row)} \\ + \text{(number of non-equivalent atom-pair blocks in one molecular pair block) namely 10} \times \text{(Sum of number of independent elements in each of the non-equivalent atom pair blocks one per LL' of the first row)} \end{array}\right\} \tag{24}$$

On the other hand one can determine the number of independent elements *via* the rules of Casella (1975). The latter scheme is useful in counterchecking that the number of independent elements derived (and their identity consequently) is correct. By numerically evaluating only the independent elements and deriving the others through table 9 reduces the computational time considerably; hence the importance of this discussion. We give in tables (10(a) and 10(b)) details of determination of the number of independent elements for the specific wavevectors of interest here.

4. Experimental

The neutron investigations are carried out using a large natural crystal of Sb_2S_3 in the form of mineral stibnite. The size of the crystal is nearly $5 \times 3 \times 1$ cm^3. For

Table 10(a). Determination of number of independent elements in the dynamical matrix *a la* Casella

	$\mathbf{q}_1$	$\mathbf{q}_2$	$\mathbf{q}_3$	$\mathbf{q}_4$
$S \in G_0(\mathbf{q})$	$h_1, h_2, h_3, h_4, h_{25}, h_{26}, h_{27}, h_{28}$	h_1, h_2, h_{27}, h_{28}	h_1, h_3, h_{28}, h_{26}	h_1, h_4, h_{26}, h_{27}
S_{-1}	$h_1, h_2, h_3, h_4, h_{25}, h_{26}, h_{27}, h_{28}$	h_3, h_{25}, h_4, h_{26}	h_2, h_4, h_{25}, h_{27}	h_2, h_3, h_{25}, h_{28}
$(S)^2$	1 1 1 1 1 1 1 1 for $r = 1$ to 8	1 1 1 1 for $r = 1$ to 4	1 1 1 1 for $r = 1$ to 4	1 1 1 1 for $r = 1$ to 4
g_q	8	4	4	4
Type	II(a)	II(a)	II(a)	II(a)
$n_r(= C_{\tau_i})$	10, 5, 5, 10, 5, 10, 10, 5	20, 10, 20, 10	15, 15, 15, 15	20, 10, 10, 20.
N_{Type} (eq. 22)	280	530 480	530	

Table 10(b). Determination of number of independent elements in the dynamical matrix according to equation (24)

	$\mathbf{q}_1$	$\mathbf{q}_2$	$\mathbf{q}_3$	$\mathbf{q}_4$
$l' \rightarrow$	1 2 3 4	1 2 3 4	1 2 3 4	1 2 3 4
No. of independent elements for equivalent atom pairs in $M(1\ l')$	4 4 4 4	5 5 8 8	6 6 6 6	5 8 8 5
No. of independent elements for non-equivalent atom pairs in $M(1\ l')$	5 5 5 5	10 10 10 10	9 9 9 9	10 10 10 10
Total no. of independent elements in $M(\mathbf{q})$	$5(4+4+4+4) \oplus 10(5+5+5+5) = 280$	530	480	530

x-ray studies three fibrils taken out at random from this crystal as well as a synthetically grown crystal were used.

The first studies were aimed at measuring low frequency TA modes polarised along ⟨010⟩ since one expected such modes to exhibit interesting features characteristic of a layered system. The experiments were carried out using a triple axis neutron spectrometer at Cirus reactor, incident neutron wavelength being fixed at 1·4 Å. A Cu(110) monochromator and a Cu(110) analyser were used. Constant **Q** and constant ΔE scans did not reveal any neutron groups associated with phonons in the measurements around (040) when search was made for TA$(00\xi/\xi00)$ modes with polarisation along *b*-axis. Instead a smoothly varying background was observed.

The 'elastic' diffraction studies indicate that one cannot identify *a* or *c* axis uniquely,

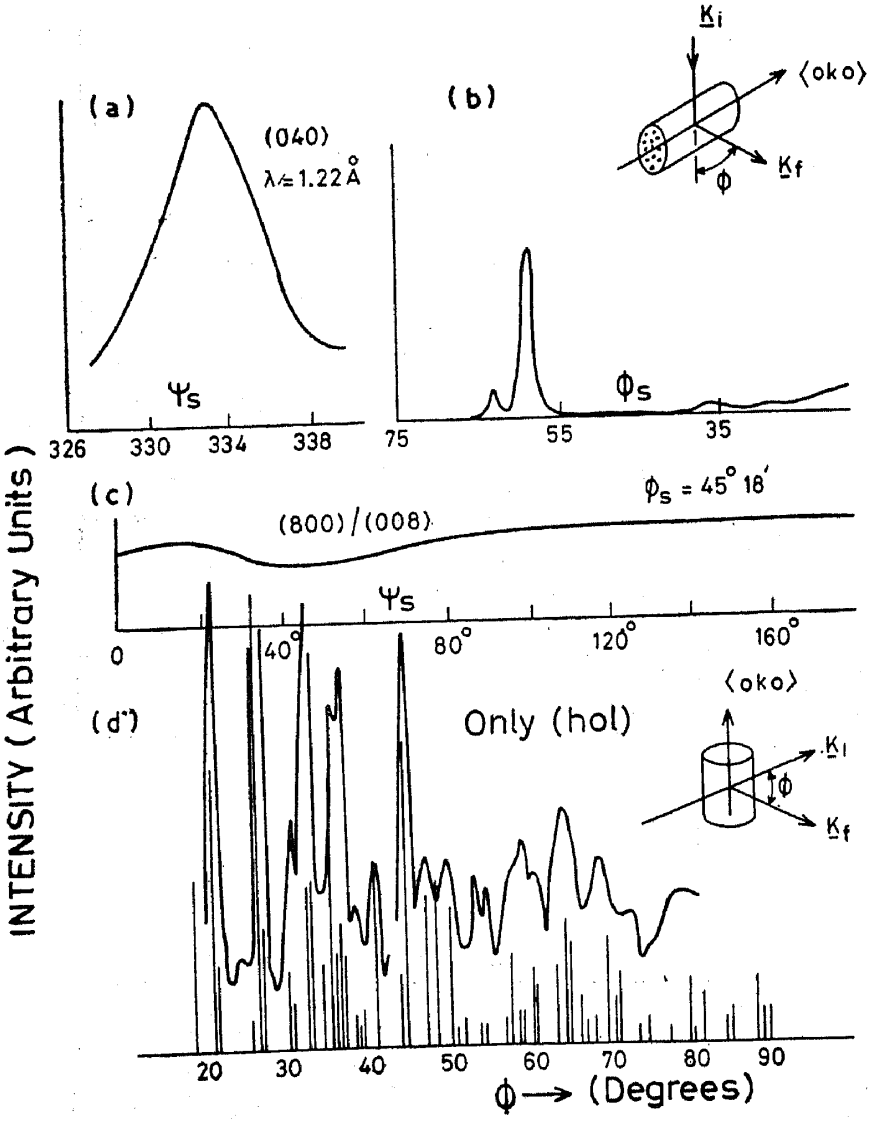

Figure 3. (a) With *b*-axis in the plane of spectrometer, a rocking curve of crystal set for (040) reflection. (b) With *b*-axis in the plane of the spectrometer, a scattering angle scan with the crystal left oriented at peak of curve given in 3(*a*). (c) With *b*-axis normal to plane of spectrometer, search for (800)/(008) reflection by crystal rocking, when detector is set for (800)/(008) reflection. (d) With *b*-axis normal to the plane of spectrometer, a scattering angle scan with the crystal left at an arbitrary orientation about *b*-axis. The vertical bars correspond to expected (*h*0*l*) reflections from a powder of Sb_2S_3.

as (h00) and (00l) reflections are always observed in the experiment. Figure 3 shows specifically the (040) Bragg peak as an example of (0k0) reflections. Rocking the crystal when the detector is set to the correct scattering angle yields a broad Bragg peak. Keeping the crystal oriented for reflection from (040) a scattering angle scan yields only the Bragg peak corresponding to (040) and nothing else as is to be expected. This was so for all (0k0) reflections examined. On the other hand a search for reflection like (800) or (008) while it gave a Bragg peak at the nominal scattering angle, a rocking of the crystal (when detector was set for the scattering angle) resulted in a continuous high intensity above background (see figure 3(c)). Secondly keeping the crystal fixed at an arbitrary orientation in the *ac* plane, a scattering angle scan yielded

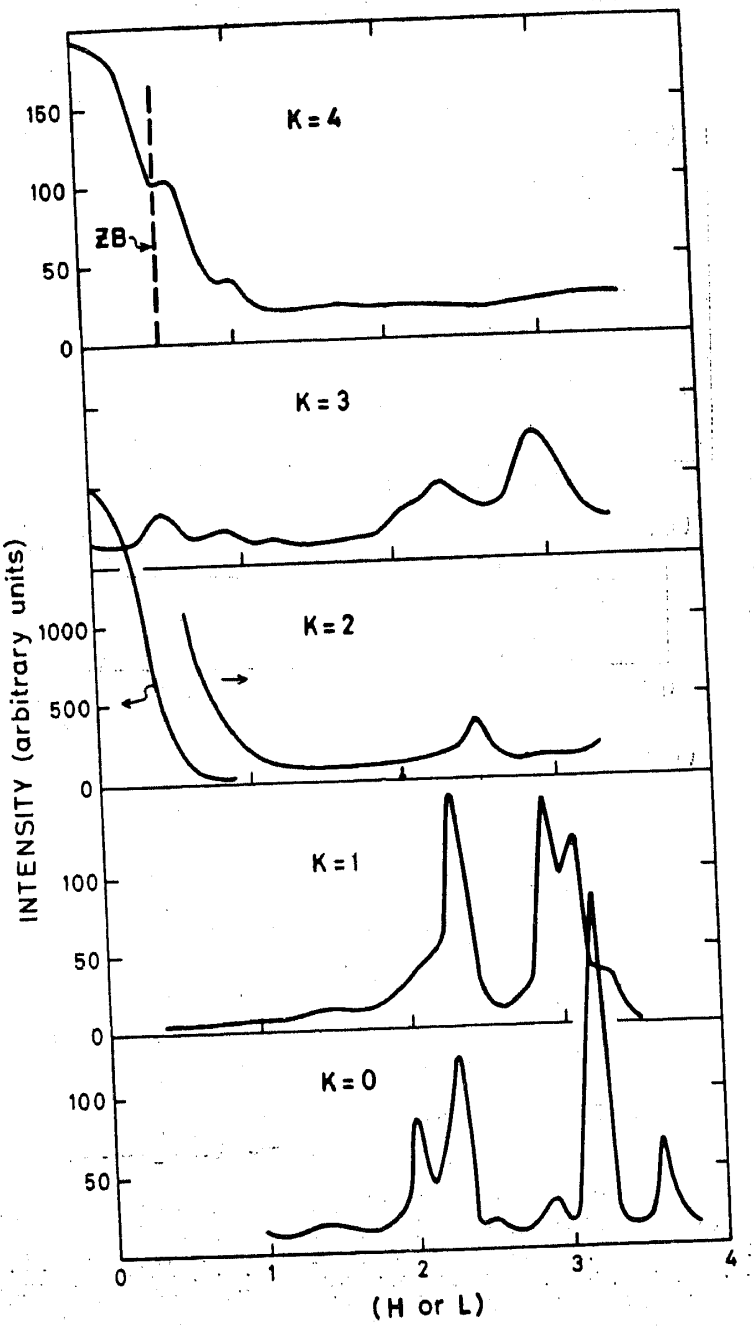

Figure 4. 'Elastic' neutron diffraction patterns from different layers along the b-axis

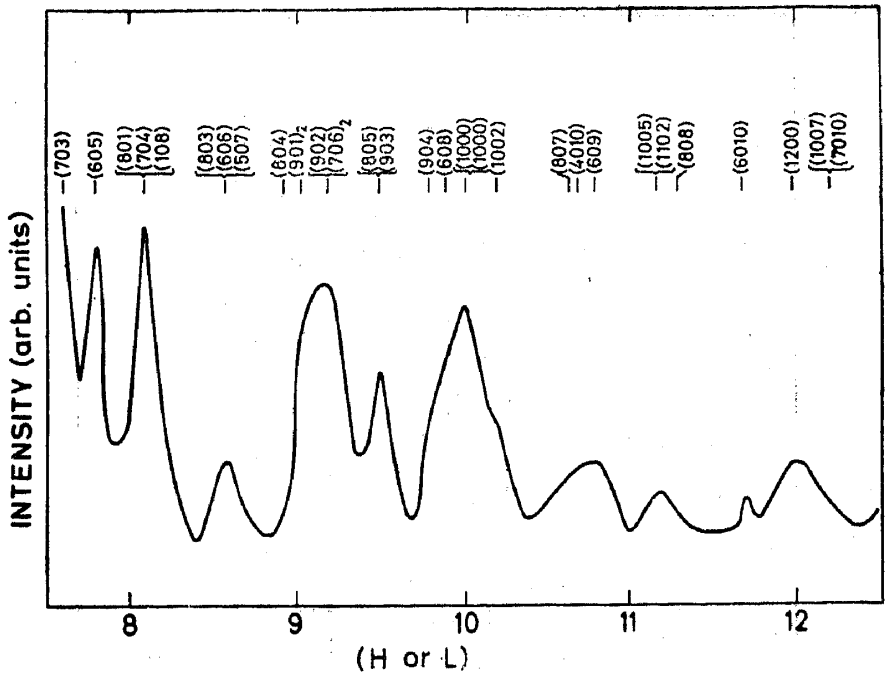

Figure 5. Zero layer data at large scattering angles. The expected (*h*0*l*) reflections are indicated in the upper part of the figure.

a pattern as if from a powder. The pattern could be indexed in terms of (*h*0*l*) reflections only. From these observations we conclude that the crystal is ordered along the *b*-axis but is disordered about the *b*-axis.

The 'elastic' neutron diffraction patterns corresponding to different (0*k*0) layers are shown in figure 4. One may notice that the Bragg peaks are extended in the reciprocal space considerably in the *ac* plane. These features resemble the 'elastic' diffraction patterns from CsD_2PO_4. (Semmingsen *et al* 1977). The zero-layer data at large scattering angle could be indexed as in figure 5.

Figure 6 shows details of the Bragg intensity around (040) lattice point. The diffuse intensity is extended in the *ac* plane and quite narrow along the *b*-axis. Such a pattern is expected of quasi-one-dimensional systems.

The x-ray diffraction patterns were studied to investigate this feature further. Mo-K_α filtered radiation was used using a x-ray generator operating at 30 kV, 40ma. Three specimens taken at random from the large crystal in the form of fibrils of thickness $\sim$0.5 mm as well as a synthetically grown crystal of similar thickness were used in these studies. Rotation photograph about *b*-axis is shown in figure 7. The large number of spots in each layer may be associated with disorder in the system. Once again we notice that the crystal is ordered along the *b*-axis. On prolonged exposures, we also notice additional diffuse lines in the rotation photographs. Returning to the neutron experiments they also revealed presence of these lines. We have not investigated the origin of these lines further. The Weissenberg pattern about *b*-axis in the zero layer is shown in figure 8. One may notice that each of the Bragg spots is associated with diffuse streaks. Figure 9 shows the nature of diffuse streaks in the Weissenberg pattern of the *a*-axis. Clearly the diffuse streaks are much less. Therefore, we note that the diffuse streaks are prominent in the *ac* plane. Such diffuse streaks could be due to static or dynamical effects.

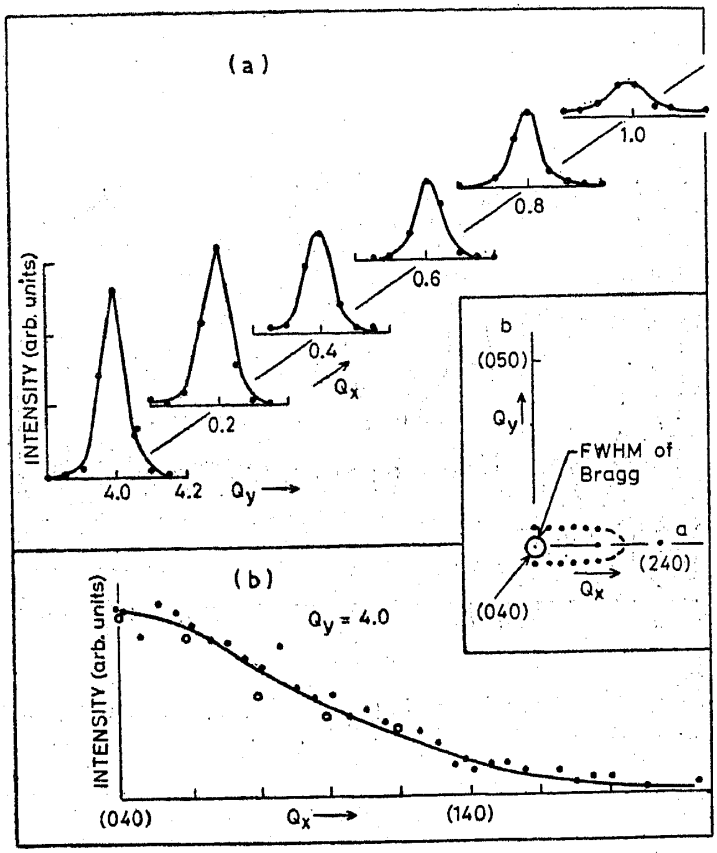

Figure 6. Diffuse 'elastic' intensity around (040) lattice point. (a) The scans along Q_y corresponding to different Q_xs. (b) Scan along Q_x for $Q_y = 0$; open circles correspond to $K = 4$ layer data of figure 5 for comparison.

The inset in the middle shows an elliptical contour corresponding to the 'base-width' of scans in (a). Note that the ellipse is extended beyond (140) along a/c and its width along the *b*-axis is only about 10% of 1/d (010).

Inelastic neutron scattering measurements alone can help to identify the real cause of the various anomalous features in the diffraction patterns discussed so far.

However, even in a second attempt to look for TA modes along a^*/c^* polarised along $\langle 010 \rangle$ we have not been successful. Only a large smoothly varying background extending from nearly $\nu = 0$ to 3 or 4 THz is seen. Measurements along the *b*-axis around (040) do indicate a few phonon modes rather weak in intensity as shown in figure 10. These phonons may be associated with longitudinal modes along $\langle 010 \rangle$. Measurements carried out at ~ 100 K did not improve the situation. 'Elastic' diffraction patterns also did not change qualitatively at this temperature.

5. Dynamical calculations

The lattice dynamics of layered crystals is generally studied using the axially symmetric force constant model in which the force constants are derived by fitting the lattice dynamical expressions to elastic constants, light scattering data and neutron data (Wakabayashi and Nicklov 1979). Generally, the range of interactions is limited to nearest neighbour and next nearest neighbours and Coloumb interactions, if any, are

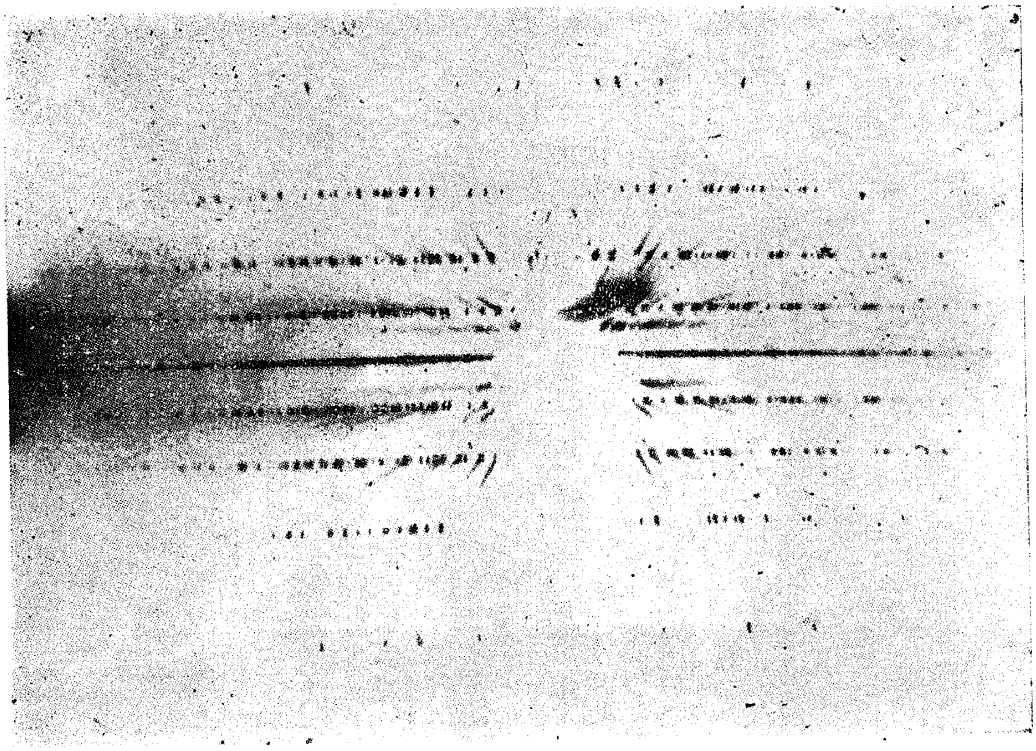

Figure 7. Rotation x-ray photograph about *b*-axis.

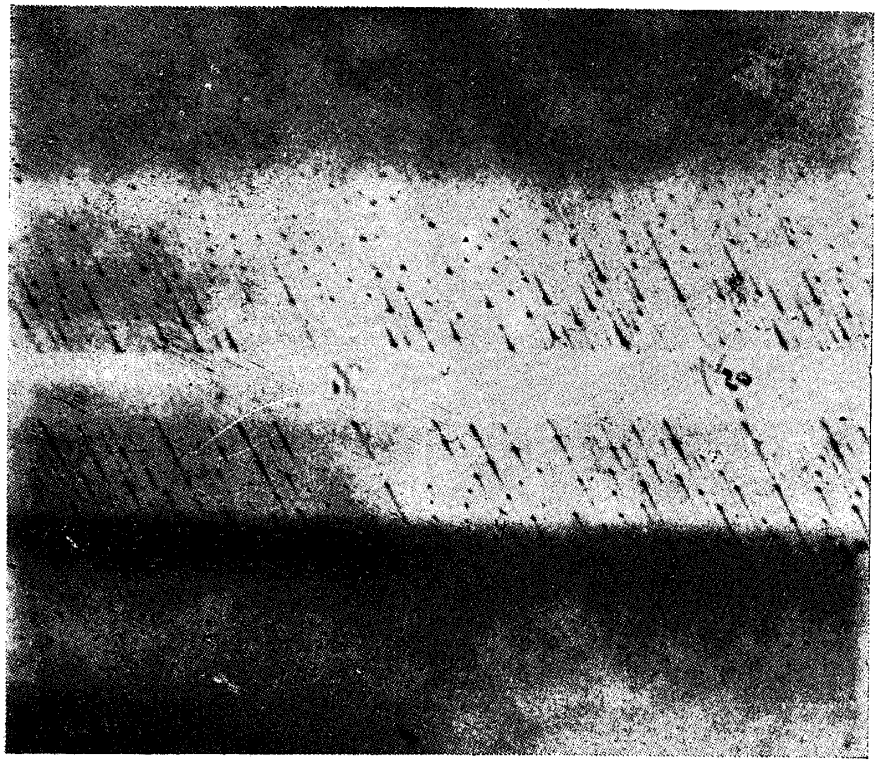

Figure 8. Weissenberg pattern about *b*-axis in the zero layer.

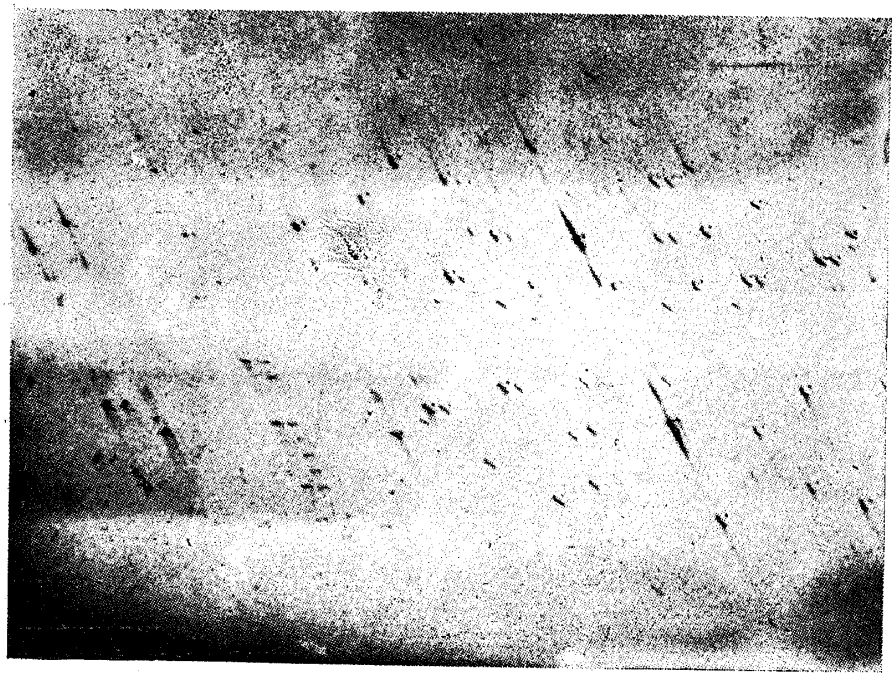

Figure 9. Weissenberg pattern about *a*-axis in the zero layer.

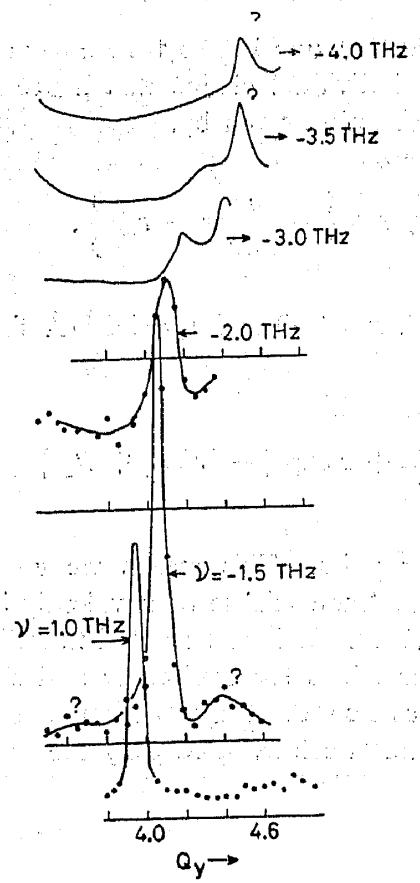

Figure 10. Phonons observed along *b*-axis around (040) by inelastic neutron scattering.

not explicitly taken into account. Once the force constant parameters are determined by least squares fitting, they are used to derive the phonon dispersion relation in high symmetry and off-symmetry directions and also to obtain frequency distribution.

We have employed a different approach for study of Sb_2S_3. Since elastic constants are not available in literature for Sb_2S_3 and since light scattering data is ambiguous, we thought it best to calculate the phonon dispersion relation using a model in which interatomic potentials are based on microscopic considerations. To begin with, we assumed that Sb_2S_3 can be treated as a partially ionic system and hence associated the interatomic pair potential to be of the form

$$V(r) = \frac{Z_1 Z_2 e^2}{4\pi\epsilon_0 r} + a \exp\{-br/(R_1 + R_2)\}, \tag{25}$$

with $a=1822$ eV and $b=12{\cdot}364$ (see also Balkanski *et al* 1971). Here Z_1 and Z_2 are charge parameters and R_1 and R_2 radii parameters associated with the atom pair whose potential is given by this equation. This simple model (a variation of the well-known rigid ion model) has been successfully used in our investigations of several complex ionic systems (Paper I and Rao and Chaplot (1979)). The potential given in (25) was used to calculate the lattice frequencies of Sb_2S_3 along the three symmetry directions Σ, Δ and Λ using the computer program DISPR (Chaplot 1978) discussed earlier in paper I. Through extensive calculations we find that the model

does not yield real frequencies in spite of variation of parameters over reasonable range. Hence we assumed that one has to take into account the strong, covalent nature of bonding within individual chains and hence reformulate the dynamical model with the potential function given by,

$$V(r) = -CD_e \exp\left\{-\frac{n}{2Cr}(r - r_0)^2\right\}, \tag{26a}$$

with $C=1{\cdot}0$, $D_e=3{\cdot}47$ eV, $n=13{\cdot}0$ and $r_0=2{\cdot}36$ Å for Sb-S pairs separated by distances less than 2·6 Å.

and $$V(r) = \frac{Z_1 Z_2 e^2}{4\pi\epsilon_0 r} + a \exp\{-br/(R_1 + R_2)\} \tag{26b}$$

same as (25) for all other pairs. This means we consider $Sb_I - S_{II}$, $Sb_I - S_{III}$ and $Sb_{II} - S_I$ pairs within a 'molecule' to be covalently bonded and all other interactions to be specified by (26b). It is to be noted that $Sb_{II} - S_{III}$ is included in the latter. The range of interactions for coulombic and short-range interactions are optimised by DISPR. As elastic constants are not available from literature and as light scattering data is ambiguous we have used only the maximum value of observed optical data (Balkanski *et al* 1971; Kartha 1981) as indicating the upper limit of lattice frequencies as a criterion to choose the parameters of the model, apart from reasonable cohesive energy of the crystal*. Potential parameters have been arrived at as described in paper I and by Chaplot (1982). The final parameters that enter the potential function 26(b) are given in table 11. We observe that, as in our study of $KNbO_3$ (Chaplot and Rao 1980, 1981) that the low frequency modes were sensitive to variations of *one* parameter; in Sb_2S_3 it is the radius parameter of Sb_{II}. This parameter was varied to ensure that all frequencies are real. The dispersion relation given in figure 11 can be taken as first order estimate to interpret experimental data but cannot be taken as absolute values for detailed comparison since there is scope to vary the model parameters to provide better estimates as experimental data become available. As already mentioned in the introduction, we have used the group theoretical results given in § 3 for checking dynamical matrix, block diagonalising the dynamical matrix for numerical solutions (the eigenvalue problem could not have been solved without block-diagonalising first to accommodate the problem within the capacity of the computer memory) and for obtaining the eigenvectors. The eigenvectors derived from the numerical calculations have been used in calculation of inelastic neutron scattering structure factors also which are of great value for any future neutron experiments.

*Now from hindsight we know that the choice of covalent nature of binding amongst Sb_{II}-S_I and Sb_I-S_{II} and Sb_I-S_{III} can be associated with the fact that the corresponding bond lengths are of the order of sum of covalent radii of atoms forming the pair and choice of ionic cum short range interaction between Sb_{II} and Sb_{III} can be associated with the fact that the corresponding bond length is of the order of sum of their ionic radii as given by Shannon and Prewitt (1969), Shannon (1976) and Shannon and Prewitt (1981). All other interactions will be non-bonded and given by the usual ionic and short range interactions. Perhaps a better choice would be to consider two different covalent functions for covalent bonds associated with Sb_I and Sb_{II}. We have not carried out numerical calculations so far with such a choice.

Table 11. Charges and radii parameters for Sb_2S_3

Parameter \ Atom	Sb_I	Sb_{II}	S_I	S_{II}	S_{III}
Charges(e)	1·2	1·2	−0·8	−0·8	−0·8
Radii (Å)	1·35	1·8	2·45	2·45	2·45

Table 12. Calculated elastic constants for Sb_2S_3 (in 10^{11} dynes/cm^2)

Elastic constant	From slopes of dispersion relations of acoustic phonon branches along $\Sigma(100)$	$\Delta(010)$	$\Lambda(001)$
C_{11}	4·72	—	—
C_{22}	—	9·34	—
C_{33}	—	—	6·33
C_{44}	—	1·96	2·32
C_{55}	3·08	—	2·43
C_{66}	0·21	0·39	—

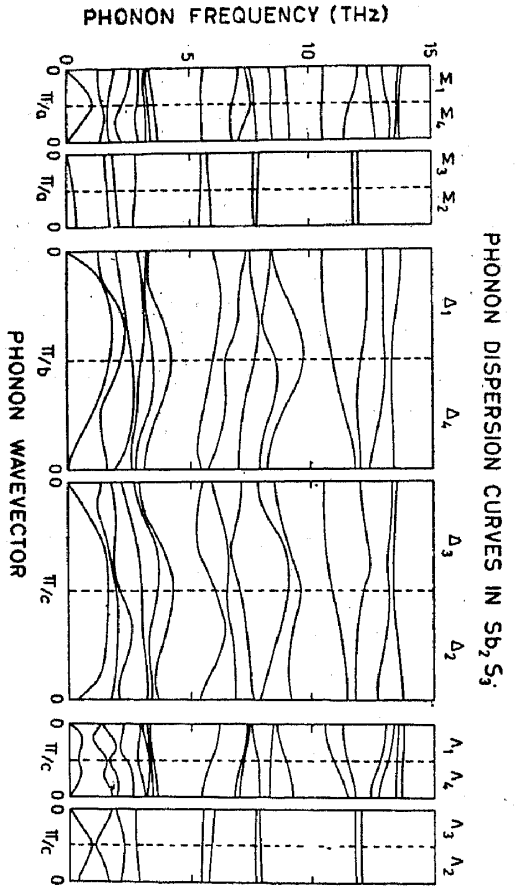

Figure 11. Theoretical dispersion curves of phonons along Σ, Δ and Λ directions in the paraelectric phase of Sb_2S_3.

6. Discussion

As discussed in § 4, experimental neutron and x-ray scattering studies have resulted in the following observations:—disorder in the *ac* plane, presence of diffuse intensity in this plane, difficulty to observe low frequency TA modes in the plane polarised along the *b*-axis and additional diffuse lines. These features can be associated with a variety of possible static (like polytypism, disorder in the crystal, incommensurable structure) or dynamic (like very low frequency TA modes that cannot be resolved from the elastic intensity, overdamped modes, etc) causes. We comment on those aspects that may be dynamical in origin as reflected in the phonon dispersion curves.

From figure 11 we note that—

(i) along Σ and Λ directions there are rather flat low frequency TA-TO modes which can give rise to diffuse scattering as in the case of $KNbO_3$. Figure 12 shows the iso-structure factor contours in the *bc* plane which substantiates this conclusion. Unless one carries out high resolution experiments one may not be able to observe these phonons clearly separated from the elastic intensity. It may be observed that the resolution of our spectrometer is rather poor and it is rather difficult to improve the resolution in view of the low flux of the reactor.

(ii) We have noted earlier in case of $KNbO_3$ (Chaplot and Rao 1980, 1981) and recently in β-KNO_3 (Chaplot 1982) that temperature/pressure dependence of lattice modes can be 'simulated' by variation of parameters of the dynamical model. Figure 13 shows the results of such parametric variation at wavevectors (0.05,0,0), (0,0.05,0) (0,0.001,0) and (0,0,0.05). One can identify the 'soft' branches that may lead to phase transitions from this figure. The lower part of the figure is an enlarged version of phonon frequencies below 0.4 THz. Along the *b*-direction, we have given results for the wave vector (0, 0.001, 0) since all the eigen frequencies are real at (0, 0·05, 0) and softening is observable only for shorter wave vectors. It is interesting to observe that the TA and TO modes along Σ direction belonging to Σ_2 and Σ_3 representations and TO mode along Λ direction of Λ_2 representation soften as a function of the parameter. We wish to point out that since the TA and TO modes at (0.05, 0, 0) are soft, the entire TA-TO branch along Σ direction is soft. The radius parameter of Sb_{II} has to be chosen so as to fit these modes in any calculation to provide correct low-frequency behaviour. The polarisation vector of this branch indicates that the two

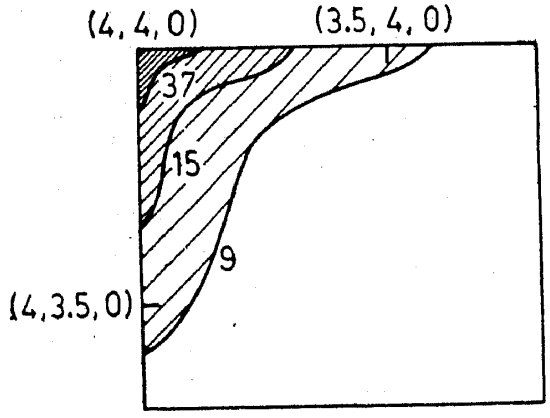

Figure 12. Dynamical structure factor contours in the *ac* plane. These contours suggest possible observation of diffuse scattering in poor resolution experiments along *a* and *c* directions.

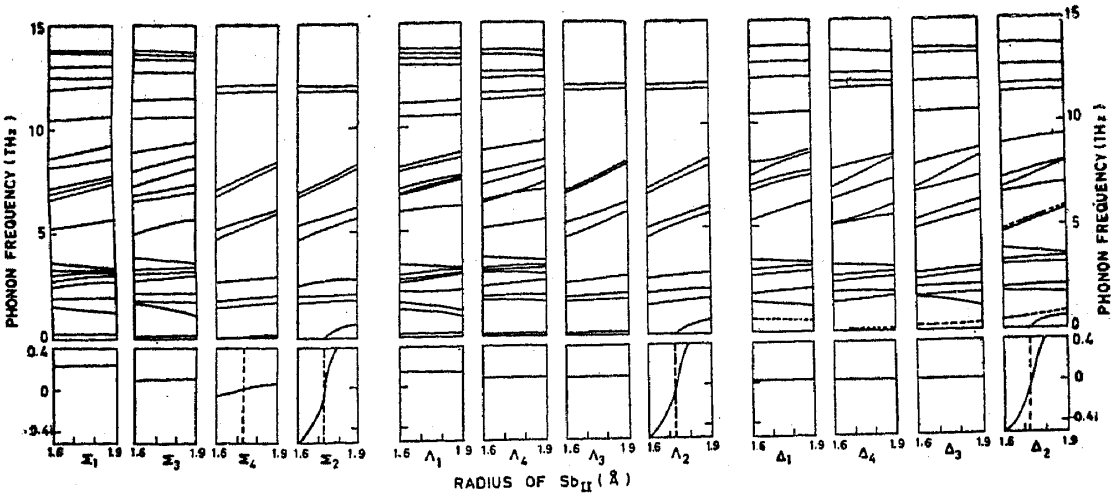

Figure 13. Theoretical changes expected in the eigen frequencies at selected wave vectors as a function of variation in the crucial radius parameter of Sb_{II}. The lower figure is an expanded version of the low frequency range of the upper figure. Note that the ordinate scale in this part of the diagram covers real and imaginary values of frequencies, although the latter is not physically meaningful. We believe that the system undergoes a non-ferroelectric phase transition as the lowest TA-TO mode becomes imaginary.

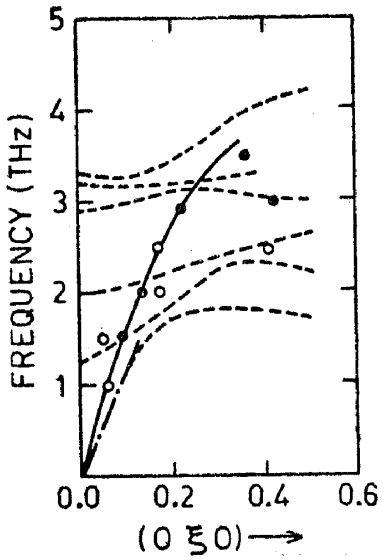

Figure 14. Dispersion curves of phonons along *b*-axis. Open circles and closed circles are data from neutron experiments. The full line is a guide to the eye through these data points. Chain line through the origin corresponds to the LA branch using theoretically evaluated elastic constants. Dashed lines are some of the theoretically expected branches in this direction.

$(Sb_4S_6)_n$ chain units take part rigidly in these vibrations along the *b*-direction (in phase at $\mathbf{q}=0$ for the TA mode progressively changing over to out-of-phase at $\mathbf{q}=0$ TO branch).

(iii) The TA-TO branches along *a* and *c* directions are almost similar in nature while those along *b*-axis are quite dissimilar, a feature related to anisotropy in the system associated with one-dimensionality.

(iv) The lowest lying zone-center TO mode in the *a* and *c* directions belongs to Γ_2 representation which is optically 'silent'. Hence we believe that the mode associated with the elastic anomaly referred in (ii) above cannot be observed by light scattering techniques. From figure 13 we observe that one of the higher frequency optically active zone-center TO modes may be responsible for ferroelectric phase transition. High resolution light scattering experiments have to be conducted to resolve the ferroelectric mode.

(v) From the slopes of the acoustic phonon branches we infer the values for elastic constants as given in table 12. The elastic constants may show anomalous behaviour as a function of temperature/pressure as seen by the parametric dependence of lattice modes (figure 13).

(vi) Finally, we compare in figure 14 the phonon data which we have experimentally derived from figure 10 with the low frequency branches along (00ξ). It is obvious that at this stage we cannot make any meaningful comment on the theoretical calculations based on this data. This points to the need of high resolution inelastic neutron scattering measurements.

7. Conclusions

With the help of lattice dynamical calculations we are able to understand some of the features of the experimental observations of Sb_2S_3 by neutron and x-ray scattering. In particular, we believe that the soft and flat TA-TO branches along *a* and *c* axes may be responsible for the diffuse streaks.

High resolution inelastic neutron scattering experiments are required to be carried out to measure the soft TA, TO and other modes in the system. The structure factors calculated using the dynamical model discussed here may help in the experiments.

Since the zone centre soft lowest TO made belongs to the optically 'silent' Γ_2 symmetry, we believe that light scattering studies are not appropriate to examine this mode.

Ultrasonic measurements are required to be carried out to confirm the predicted softening of the elastic constant.

Acknowledgements

The authors are grateful for the kind encouragement and interest in this work by Drs P K Iyengar and N S Satya Murthy. Useful discussions with Drs V C Sahni, U R K Rao and V B Kartha are gratefully acknowledged.

Appendix

Crystallographic structural references and especially that of McKee and McMullan (1976) indicate that above 17.5 C, Sb_2S_3 is in the paraelectric phase and hence D_{2h}^{16} is the appropriate space group. This conclusion is based on a work due to Grigas and Karpus (1968) which stated that there is a *first order* phase transition at 17.5 C to a ferroelectric phase.

The lattice dynamical results have relevance to infrared and Raman spectra and therefore comparison with such and other related work is in order. The paper by Grigas *et al* (1976) deals with measurement of dielectric permittivity and dielectric non-linearity at micro-wave range in Sb_2S_3. In these measurements one deals with reflection coefficients of microwaves in a cavity in which Sb_2S_3 crystals are placed and one derived ϵ values from the reflection coefficients as a function of temperature. The results are believed to indicate 'diffuse' phase transitions in the range of 290-310 K and 420-450 K. The authors have concluded that Sb_2S_3 is polar below 420K (space-group C_{2v}) and non-polar above. They also state that the hysteresis loops observed (Orliukas and Grigas 1974) as well as effects of pressure on dielectric properties and domain structure (Kachalov *et al* 1975) imply that Sb_2S_3 is ferro-electric below 450K and undergoes *second order* phase transitions. Petzelt and Grigas (1973) have also studied far infrared dielectric dispersion in Sb_2S_3 and isomorphous compounds Bi_2S_3 and Sb_2Se_3. Their approach has been to count the number of modes that are 'visible' and associate this number with the number of modes expected in D_{2h} and C_{2v} symmetries. Their results were as follows:

	Expected no. of IR modes if space group symmetry were		Observed (IR)		
	D_{2h}	C_{2v}	Sb_2S_3	Bi_2S_3	Sb_2Se_3
Elle	4	10	3–13	3–10	3–5
Ella	8	13	9–13	9–12	8
Ellb	8	13			

'These data',-according to the authors-, 'indicate that Sb_2S_3 and Bi_2S_3 are compatible with both symmetries'. However the authors also state that 'the great number of observed peaks in Sb_2S_3 in comparison with other compounds supports the C_{2v} symmetry in the whole temperature regime (100–400K?) investigated. Bi_2S_3 is probably less polar than Sb_2S_3 while in Sb_2Se_3 the symmetry is very probably non-polar'. The authors, in view of their microwave absorption experiments conclude that the 490-450K dielectric anomaly is associated with $D_{2h} \rightarrow C_{2v}$ symmetry change and 310-290K anomaly to be associated with a new kind of phase transition without symmetry change (or with a change $C_{2v} \rightarrow C_2$) as given in Fridkin (1980, p. 139).

In a series of differential thermal analysis experiments carried out in our laboratories no anomalies could be observed in the 100-450 K range (Rao 1981).

Clearly the situation demands a reevaluation of direct structural data to set at rest the confusion that prevails in the literature. In passing it may be noted however that Grigas and coworkers do not comment on their own observation of first order phase transition at 17.5 C in their subsequent papers.

References

Balkanski M, Teng M K, Shapiro S M and Ziolkiewicz M K 1971 *Phys. Status Solidi* **44** 355
Bayliss P and Nowacki W 1972 *Z. Krist.* **135** 308
Bohae P and Kaufmann P 1975 *Mater. Res. Bull.* **10** 613
Casella R 1975 *Phys. Rev.* **11** 4795
Casella R 1975 *Phys. Rev.* **12** 4573

Chaplot S L 1978 BARC Report 972
Chaplot S L 1982 Ph.D. Thesis (Bombay University)
Chaplot S L and Rao K R 1980 *J. Phys.* **C13** 747
Chaplot S L and Rao K R 1981 *Nucl. Phys. Solid State Physics Sym. (India)* **C24** 209
Fridkin V M 1980 *Ferroelectric semiconductors* (New York: Consultants Bureau)
Grigas J 1978 *Ferroelectricity* **20** 173
Grigas J and Karpus 1968 *Sov. Phys. Cryst.* **12** 627
Grigas J, Meshkauskas J and Orliukas A 1976 *Phys. Status Solidi* **37** K39
Hoffmann W 1933 *Z. Krist.* **86** 225
Kachalov N P, Orliukas A, Polandov I N and Grigas J 1975 *Fiz. Tverd. Tela* **17** 1790
Kartha V B 1981 Private Communication
Kovalev O V 1965 *Irreducible representations of space groups* (New York: Gordon & Breach)
Maradudin A and Vosko S H 1968 *Rev. Mod. Phys.* **40** 1
McKee D O and McMullan J F 1975 *Z. Krist.* **142** 447
Orliukas A and Grigas J 1974 *Kristallographia* **19** 880
Petzelt J and Grigas J 1973 *Ferroelectrics* **5** 59
Rao U R K (1981) Private Communication
Rao K R and Chaplot S L 1979 in *Current trends in lattice dynamics* (ed) K R Rao (Bombay: Indian Physics Association) p. 705
Rao K R, Chaplot S L, Iyengar P K, Venkatesh A H and Vijayaraghavan P R 1978 *Pramana* **11** 251 (referred to as Paper I in text)
Scavnicar S 1960 *Z. Krist.* **114** 85
Shanon R D 1976 *Acta Crystallogr.* **A32** 751
Shannon R D and Prewitt C T 1969 *Acta Crystallogr.* **B25** 925
Shanon R D and Prewitt C T 1981 *Current Contents* No. 21 p. 18
Sieskind M 1978 *J. Phys. Chem. Solids* **39** 1251
Semmingsen D, Ellenson W D, Frazer B C and Shirane G 1977 *Phys. Rev. Lett.* **38** 1299
Wyckoff R W G 1948 *Crystal Struct.* **1** Chap. 5 p. 9
Wyckoff R W G 1958 *Crystal Struct.* **2** 27
Wieting T J and Schluter M 1979 *Electrons and phonons in layered crystal structures* (Drodrecht: D Reidel Publ. Co.)
Venkataraman G and Sahni V C 1970 *Rev. Mod. Phys.* **42** 409
Wakabayashi N and Nicklov R M 1979 in *Electrons and phonons in layered crystal structures*, (ed) T J Wieting and M Schluter p. 409